

University of Windsor

## Scholarship at UWindor

---

Electronic Theses and Dissertations

Theses, Dissertations, and Major Papers

---

2004

### Frequency dependent dielectric constants and its numerical computation through Kramers-Kronig relations and Hilbert transform.

Ruwan D. Weerasundara  
*University of Windsor*

Follow this and additional works at: <https://scholar.uwindsor.ca/etd>

---

#### Recommended Citation

Weerasundara, Ruwan D., "Frequency dependent dielectric constants and its numerical computation through Kramers-Kronig relations and Hilbert transform." (2004). *Electronic Theses and Dissertations*. 2158.

<https://scholar.uwindsor.ca/etd/2158>

This online database contains the full-text of PhD dissertations and Masters' theses of University of Windsor students from 1954 forward. These documents are made available for personal study and research purposes only, in accordance with the Canadian Copyright Act and the Creative Commons license—CC BY-NC-ND (Attribution, Non-Commercial, No Derivative Works). Under this license, works must always be attributed to the copyright holder (original author), cannot be used for any commercial purposes, and may not be altered. Any other use would require the permission of the copyright holder. Students may inquire about withdrawing their dissertation and/or thesis from this database. For additional inquiries, please contact the repository administrator via email ([scholarship@uwindsor.ca](mailto:scholarship@uwindsor.ca)) or by telephone at 519-253-3000ext. 3208.

**FREQUENCY DEPENDENT DIELECTRIC  
CONSTANTS AND ITS NUMERICAL COMPUTATION  
THROUGH KRAMERS-KRONIG RELATIONS AND  
HILBERT TRANSFORM**

By

Ruwan D. Weerasundara

A Thesis

Submitted to the Faculty of Graduate Studies and Research Through the Department of  
Electrical and Computer Engineering in Partial Fulfillment of the Requirements for the  
Degree of Master of Applied Science at the University of Windsor

Windsor, Ontario, Canada  
2003



National Library  
of Canada

Bibliothèque nationale  
du Canada

Acquisitions and  
Bibliographic Services

Acquisitons et  
services bibliographiques

395 Wellington Street  
Ottawa ON K1A 0N4  
Canada

395, rue Wellington  
Ottawa ON K1A 0N4  
Canada

*Your file* *Votre référence*  
*ISBN: 0-612-92507-2*  
*Our file* *Notre référence*  
*ISBN: 0-612-92507-2*

The author has granted a non-exclusive licence allowing the National Library of Canada to reproduce, loan, distribute or sell copies of this thesis in microform, paper or electronic formats.

L'auteur a accordé une licence non exclusive permettant à la Bibliothèque nationale du Canada de reproduire, prêter, distribuer ou vendre des copies de cette thèse sous la forme de microfiche/film, de reproduction sur papier ou sur format électronique.

The author retains ownership of the copyright in this thesis. Neither the thesis nor substantial extracts from it may be printed or otherwise reproduced without the author's permission.

L'auteur conserve la propriété du droit d'auteur qui protège cette thèse. Ni la thèse ni des extraits substantiels de celle-ci ne doivent être imprimés ou autrement reproduits sans son autorisation.

---

In compliance with the Canadian Privacy Act some supporting forms may have been removed from this dissertation.

Conformément à la loi canadienne sur la protection de la vie privée, quelques formulaires secondaires ont été enlevés de ce manuscrit.

While these forms may be included in the document page count, their removal does not represent any loss of content from the dissertation.

Bien que ces formulaires aient inclus dans la pagination, il n'y aura aucun contenu manquant.

# Canada

© 2003 RUWAN WEERASUNDARA

## Abstract

The dielectric constant and loss are important (real and imaginary components) properties of interest to electrical engineers because these two parameters, among others, decide the suitability of a material for a given application.

The nature of some physical important parameters is such that frequency dependent real and imaginary components cannot be specified independently from each other. The Kramers-Kronig relations provide the coupling between real and imaginary components.

Occasions arise when only one of the components can be readily obtained from theoretical or experimental procedures.

The mathematical technique used by Kramers-Kronig relations, which allows one component to be defined in terms of the other is Hilbert transform since  $\varepsilon'(\omega)$  and  $\varepsilon''(\omega)$  can be shown to be Hilbert transform pairs.

The practical formation of this Hilbert transform pair is not an easy task in most instances. One cannot produce an analytical function in order to obtain its Hilbert transformation over a large frequency range.

An efficient algorithm is developed to obtain the complex dielectric permittivity of materials over a large frequency range. In this thesis, the algorithm has been verified for both theoretically generated data (Debye equation) and measured data for various high temperature dielectric materials.

This procedure calculates the one component of the dielectric constant from its other component by use of the Hilbert transform properties of Kramers – Kronig relation and FFT techniques.

Different laboratory equipments and measuring techniques were used in this project and described in detail.

## Acknowledgments

I would like to express my deepest gratitude and sincere appreciation to the graduate studies supervisor Dr. Gorur G. Raju for his guidance, advice and financial support through out my studies and research work. His interest this research and many fruitful discussions were instrumental in its successful conclusion.

I would also like to thanks Dr. Chuhong Chen and Dr. Faouzi. Ghrib for their constructive comments.

Further I would like to thanks Dr. Shervin Erfani and Mrs. Shelby Marchand for their administrative help and also Dr. Mansoor Kabir for his valuable comments on signal processing theory.

I would also like to thank Mr. Alen Jones, Mr. Don Tersigini and Frank Cicchello for helping my laboratory work.

Finally I would like to thank my wife Prasanthie and family for their valuable support and encouragement.

## TABLES OF CONTENTS

Abstract	iv
Acknowledgements	v
List of Tables	ix
List of Figures	x

### Chapter 1

#### Fundamentals of Dielectric Properties

1.1	Complex permittivity	1
1.2	Polarization	3
1.3	Polarization mechanisms	4
1.3.1	Orientational Polarizations	5
1.3.2	Ionic Polarization	5
1.3.3	Interfacial Polarization	6
1.3.4	Electronic Polarization	6
1.3.5	Frequency effects	6
1.4	Debye equations	8
1.5	Cole- Cole Relaxation	10
1.6	Davidson-Cole Equation	11
1.7	Havriliak and Negami Dispersion	11
1.8	Kramers- Kronig Relation	12

### Chapter 2

#### Numerical Computation of Dielectric Permittivity

2.1	Fourier Transform	13
2.2	Symmetry Properties of Fourier Transform	
	Applicable in this Study	13
2.3	Convolution Operation	13
2.4	Hilbert Transform	15

2.5	Proof of $\varepsilon'(\omega)$ and $\varepsilon''(\omega)$ are indeed of Hilbert Transforms each other	16
2.6	Flow Chart of the Operation	16
2.7	Application of Hilbert Transform Technique	17
2.8	Numerical Computation of Fourier Transforms	18
2.9	DFT to Compute the Continues Fourier transforms	19
2.10	Implementation Procedure	20

### Chapter 3

#### Laboratory Measurement

3.1	Measurement of Dielectric Properties	21
3.2	Available Methods for Measurement of Dielectric Properties	21
3.3	Dielectric Property Measurement Principal	22
3.4	Electrode Arrangements	23
3.5	Experimental Apparatus used for Dielectric Properties Measurement	25
3.5.1	Environmental Test Chamber	25
3.5.2	Keithely model LCZ 3330 Meter	26
3.5.3	Multi Frequency- Hp-4275 (LCR) Meter	28
3.6	Experimental set up for Dielectric Measurements	28

### Chapter 4

#### Measurement of Dielectric Properties at Low Frequency

4.1	Measurement of Charging and Discharging Currents to Obtain Dielectric Properties	31
4.2	Experimental Measurements	34
4.3	Sample Preparation and Electrodes	35
4.4	Apparatus used for Measurements	37
4.4.1	High Voltage d .c. Generator	37
4.4.2	Tenny Junior Environmental Chamber	37
4.4.3	Keithley 617C Electrometer	37



4.5	Experimental Procedure	38
4.6	Charging / Discharging Current	39
4.7	Low Frequency Dielectric Loss Factor	39
<b>Chapter 5</b>	<b>Investigated Dielectric Materials</b>	
5.1	Investigated Dielectric Materials and their electrical Properties	46
5.2	Applications	48
5.3	Electrical Properties	48
5.4	Semicrystalline Polychlorotrifluoroethylene (PCTFE)	52
	5.4.1 Chemical Structure	52
	5.4.2 Properties	52
5.5	Applications	53
5.6	Chemical Resistance	53
<b>Chapter 6</b>	<b>Results</b>	
6.1	Comparison with Theoretical Debye Curves	55
<b>Chapter 7</b>	<b>Conclusion and Recommendation for future work</b>	60
<b>Appendix</b>		61
<b>References</b>		64
<b>Vita Auctoris</b>		68

## LIST OF TABLES

TABLE		PAGE
3.1	Experimental Methods for the Measurement of Dielectric Properties	21
3.2	Specifications of Tenney Jr. Environmental Test Chamber	26
3.3	Specifications of Keithley Model LCZ 3330 Meter	27
3.4	Specifications of HP- 4275A Multi-frequency LCR Meter	28
5.1	Typical Electrical Properties Aramid Paper	49

## LIST OF FIGURES

FIGURE	PAGE
1.2 Schematic Representation of the Different Polarization Mechanisms	4
1.3 Contribution of the Different Polarization Mechanisms to the Frequency Dependence of the Relative Permittivity	9
1.4 Schematic Representation of Debye Equations Plotted as a Function of Frequency	10
1.5.1 Real Part of $\epsilon^*$ in a Polar Dielectric according to Cole-Cole	11
1.5.2 Imaginary Part of $\epsilon^*$ in a Polar Dielectric according to Cole-Cole	11
2.1 Representation of an even Function	14
2.2 Representation of an Odd Function	14
3.1 Parallel Plate Capacitor Containing a Dielectric Material and its Equivalent Circuit	22
3.2 Schematic representation of Electric Fringing Effect of an Unguarded Parallel Plate Capacitor	24
3.3 Three Terminal Electrode Arrangement	24
3.4 Front View of Keithely Model LCZ 3330 Meter	27
3.5 A Schematic Diagram of the experimental Set up Consisting of Analyser	29
4.1 Experimental Set up for the Study of Charging and Discharging Currents	34
4.2 Three Terminal Electrode Assembly	36
4.3 Thermal Protocol Adapted for Study of Charging and Discharging Currents	38
4.4 Charging Currents in Aromatic Polyamide for 10 MV/m (Nomex 410)	40
4.5 Charging Currents in Aromatic Polyamide for 6 MV/m (Nomex 410)	41
4.6 Discharging Currents in Aromatic Polyamide for 6 MV/m (Nomex 410)	42
4.7 Discharging Currents in Aromatic Polyamide for 10MV/m (Nomex 410)	43
4.8 Dielectric Loss ( $\epsilon''$ ) at very low Frequencies (T= 50, 100, 150°C)	44
4.9 Dielectric Loss ( $\epsilon''$ ) at very low frequencies (T= 200°C)	45
5.1 Nomex Type 410	46

5.2	Dielectric Properties of 0.125 mm Nomex 410 ( $\epsilon'$ )	50
5.3	Dielectric Properties of 0.125 mm Nomex 410 ( $\epsilon''$ )	51
5.3.1	Atomic Structure of PCTFE	52
5.4	Dielectric Properties of Semi Crystalline Polychlorotrifluoroethylene (PCTFE)	54
6.1	Computation of imaginary part of the Dielectric Constant from its real part (N= 8162)	56
6.2	Computation of imaginary part of the Dielectric Constant from its real part (N= 16324)	57
6.3	Computation of $\epsilon'$ from $\epsilon''$ (Nomex 410)	58
6.4	Dielectric Properties of PCTFE at 0°C	59

## CHAPTER 1

### FUNDAMENTAL OF DIELECTRIC PROPERTIES

The dielectric properties of a material are defined by permittivity  $\epsilon$ , loss factor  $\epsilon''$ , and dielectric strength. The permittivity is related to the ability to store charge and there by increase vacuum capacitance. For this a dielectric material must contain localized charge that can be displaced by the application of an electric field. This charge displacement is referred to as polarization. Such a charge displacement is time dependent in most materials, and a complex permittivity is required to adequately describe the system,  $\epsilon^* = \epsilon' + j\epsilon''$  [1]

Since the polarization mechanisms that occur in these materials depend on frequency, temperature and chemical composition, complex permittivity also depends on these parameters.

#### 1.1 COMPLEX PERMITTIVITY

Consider a capacitor that consists of two plane parallel electrodes in a vacuum having an applied alternating voltage represented by the equation.

$$V = V_m \cos \omega t \quad [1.1]$$

Where, V is the instantaneous voltage,

$V_m$  is the maximum value of V and  $\omega = 2\pi f$  is the angular frequency in rad/s.

The current thorough the capacitor  $i_L$  is given by

$$i_L = I_m \left( \cos \omega t + \frac{\pi}{2} \right) \quad [1.2]$$

$$\text{Where } I_m = \frac{V_m}{Z} = \omega C_0 V_m \quad [1.3]$$

In this equation  $C_0$  is the vacuum capacitance.

In an ideal dielectric current leads the voltage by  $90^\circ$  and there is no component of the current in phase with the voltage. If a material of dielectric constant  $\epsilon$  is now placed between the plates the capacitance increases to  $C_0\epsilon$  and the current is given by

$$i_2 = I_m \cos\left[\omega t + \left(\frac{\pi}{2} - \delta\right)\right] \quad [1.4]$$

Where  $I_m = \omega C_0 \epsilon V_m$  [1.5]

The current phasor will not now be in phase with the voltage, but by an angle  $(90-\delta)$  where  $\delta$  is called the loss angle. ( Fig 1.1 )

The dielectric constant is a complex quantity represented by

$$\epsilon^* = \epsilon' - j\epsilon'' \quad [1.6]$$

The current can be resolved into two components. The component in phase with the applied voltage is  $I_x = v\omega\epsilon''C_0$  and the component leading the applied voltage by  $90^\circ$  is  $I_y = v\omega\epsilon'C_0$

This component is the charging current of the ideal capacitor.

The component in phase with the applied voltage gives rise to dielectric loss.  $\delta$  Is the loss angle and is given by,

$$\delta = \tan^{-1}\left(\frac{\epsilon''}{\epsilon'}\right) \quad [1.7]$$

$\epsilon''$  Is usually referred to as the loss factor and  $\tan\delta$  is the dissipation factor.

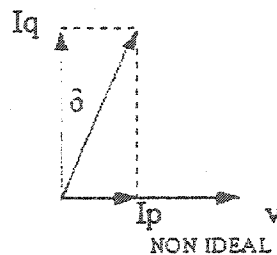


**Figure 1.1 Definition of loss angle**

The dielectric properties discussed are related to the polarizability of a material by,

$$P = (\epsilon' - 1)\epsilon_0 E \quad [1.8]$$

Where  $P$  is the Polarization in a material

$\epsilon'$  is the real part of permittivity

$E$  is the electric field strength

$\epsilon_0$  is the permittivity of free space [1]

As a result an understanding of the mechanisms of polarization that can occur in materials is necessary to understand the dielectric properties of these materials.

## 1.2 POLARIZATION

The dielectric constant of a material is an interesting parameter only if the material is exposed to an electric field. The effect of an electric field can be two fold.

- (a) It induces electric dipole in the material and tries to align them in the field direction.
- (b) It tries to align dipoles that are already present in the material. In other words material contains electric dipoles even without a field.

Under a.c. conditions electric field may change the distribution of an existing dipoles while trying to align them. It may generate new dipoles and different arrangements.

Therefore the dipole arrangement will change as a function of frequency and hence the change of dielectric constant.

### 1.3 Polarization Mechanisms

Polarization mechanisms that occur in dielectric materials are Orientational polarization, Ionic polarization, Interfacial polarization, and Electronic polarization, figure 1.2. [1].

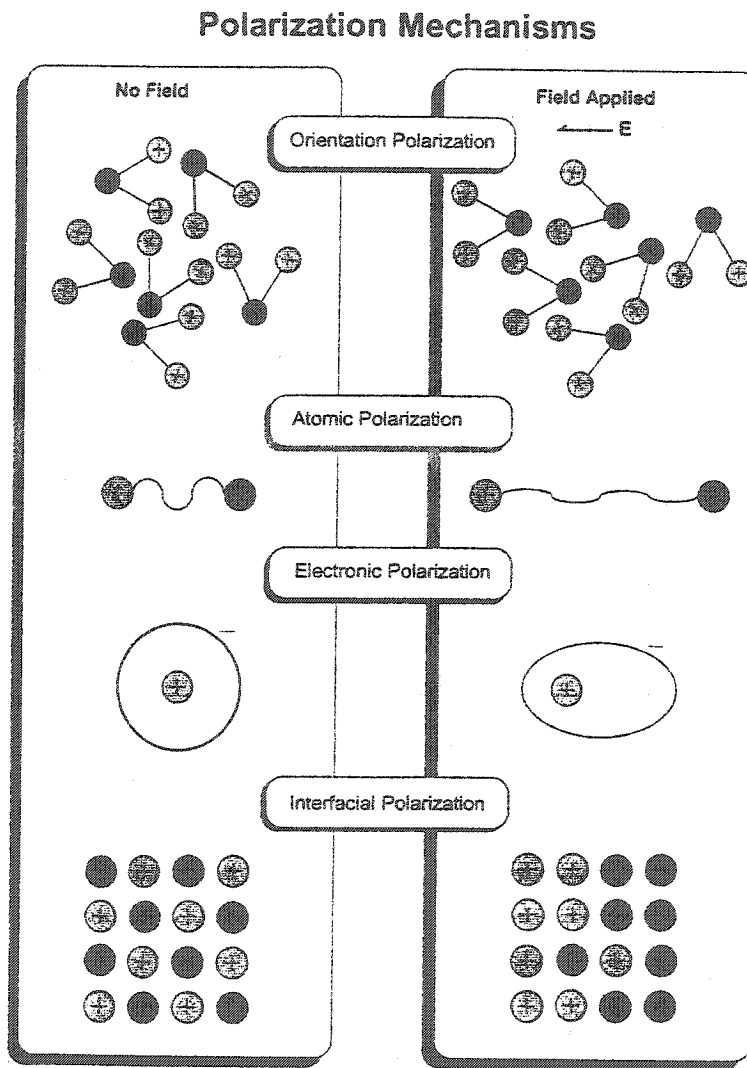


**Figure 1.2 . Schematic Representation of the Different Polarization Mechanisms [29]**



The addition of an applied field to each of the situations shown on the left of figure 1.2 will cause a displacement of charge and thus affect the dielectric constant by effectively cancelling a part of the applied field. In a given dielectric material the total polarization,  $P$  is the sum of the polarization resulting from each mechanism.

### 1.3.1 ORIENTATIONAL POLARIZATION

The rearrangement of electrons when some molecules from can create a dipole moment in the resulting molecule. When no electric field is present the molecules are randomly orientated and no net charge exists in the material. However, when a field is applied the dipoles will rotate cancelling part of the applied field and leading to an orientation polarization. This process must depend upon the temperature and excitation frequency of a given system.

### 1.3.2 IONIC POLARIZATION

In this case a (solid) material must have some ionic character. It then automatically has an internal dipoles exactly cancel each other and are unable to rotate.

The external field then induces net dipoles by slightly displacing the ions from their rest position. The paradigmatic materials are all simple ionic crystals like Sodium Chloride. (NaCl.)

### 1.3.3 INTERFACIAL POLARIZATION

Electrically heterogeneous materials may experience interfacial polarization. In these materials the motion of charge carriers may occur more easily through one phase and therefore are constricted at phase boundaries. As a result charges build up at interfaces and can be polarized in an applied field. This effect often depends greatly on the conductivities of the phase present.

All these polarization mechanisms can exist in homogenous pure materials, with the exception of interfacial polarization, which must contain either multiple phases or mixtures of pure materials to exist. Additional polarization mechanisms may occur when mixtures of materials are present.

### 1.3.4 ELECTRONIC POLARIZATION

When the atom is situated in an electric field the charged particles experience an electric force as a result of which the centre of the negative charge cloud is displaced with respect to the nucleus. A dipole moment is induced in the atom and the atom is said to be electronically polarized.

### 1.3.5 FREQUENCY EFFECTS

The various polarization mechanisms vary with frequency in different ways. The relative permittivity  $\epsilon'$  will be controlled by different mechanisms as the frequency changes. This is reflected by the strong variation of  $\epsilon'$  with frequency schematically represented in fig (1.3)

The frequency dependent response is due to several factors. For electronic and atomic polarization the inertia of electrons must be accounted for. Due to this inertia effect these polarization mechanisms will be small for any frequency other than the resonant frequency. Below this frequency little contribution to  $\epsilon'$  and  $\epsilon''$  is given from these mechanisms. At the resonant frequency a peak in  $\epsilon''$  will occur and dispersion will occur in  $\epsilon'$  [2]

Materials, which undergo orientation polarization, will experience dispersion at the relaxation frequency. In these materials a large change in  $\epsilon'$  and  $\epsilon''$  will occur at this frequency. At the relaxation frequency the oscillation of the applied field is "too fast" for the molecules to have time to fully rotate. As a result,  $\epsilon'$  will decrease when the relaxation frequency is reached since there is less interaction of the field with the dipoles, as the frequency is increased.

A peak in  $\epsilon''$  also occurs at this frequency since the energy is dissipated in the process. This is due to the fact that at low frequencies rotation is slow, minimal energy is dissipated and above the relaxation frequency the molecules only rotate a small distance, so again minimal energy is dissipated. The maximum lies in between these two extremes at the relaxation frequency.

A relaxation of this type can be described by the Debye [3] equations in polar materials.

#### 1.4 DEBYE EQUATIONS

Debye derived the equation for complex permittivity as,

$$\epsilon^* = \frac{(\epsilon_s - \epsilon_\infty)}{(1 + j\omega\tau)} \quad [1.9]$$

Where,

$\epsilon_s$  = Dielectric constant under direct voltage

$\epsilon_\infty$  = Dielectric constant at infinity frequency

$\omega$  = Angular frequency

$\tau$  = Relaxation time

$\epsilon^*$  = Complex dielectric constant

From this we have,

$$\epsilon' = \epsilon_\infty + \frac{(\epsilon_s - \epsilon_\infty)}{(1 + \omega^2\tau^2)} \quad [1.10]$$

$$\epsilon'' = \frac{(\epsilon_s - \epsilon_\infty)\omega\tau}{(1 + \omega^2\tau^2)} \quad [1.11]$$

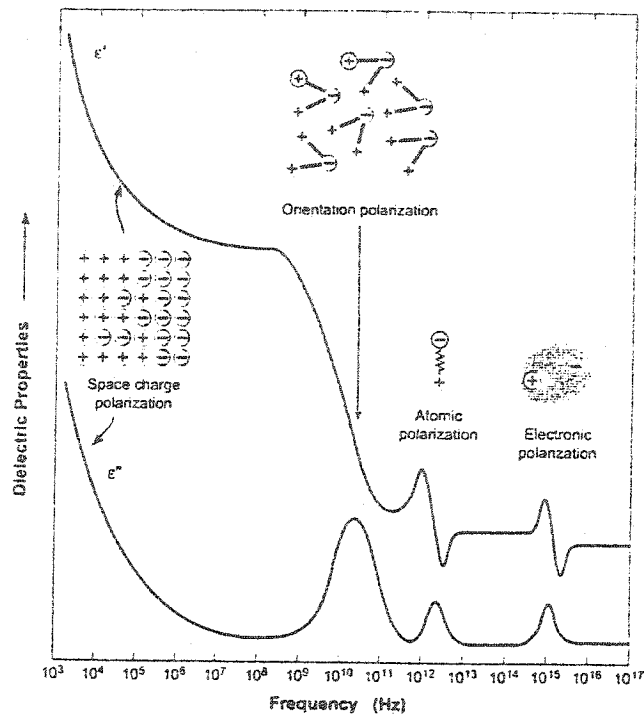


**Figure 1.3. Contribution of the Different Polarization Mechanisms to the Frequency Dependence of the Relative Permittivity [29]**

An examination of these equations shows the following characteristics.

- (1) For small values of  $\omega\tau$  the real part  $\epsilon' \approx \epsilon_s$ , because of the squared term in the denominator of equation [1.10] and  $\epsilon''$  is also small for the same reason. At  $\omega\tau = 0$  we get  $\epsilon'' = 0$  as expected because this is D.C. Voltage.
- (2) For very large values of  $\omega\tau$ ,  $\epsilon' = \epsilon_\infty$  and  $\epsilon''$  is small.
- (3) For intermediate values of frequencies  $\epsilon''$  is a maximum when  $\omega_p\tau = 1$ .

Where,  $\omega_p$  is the angular frequency at which the peak occurs.

Variation of  $\epsilon'$  as a function of frequencies is referred to as dispersion in the literature on dielectrics. Variation of  $\epsilon''$  as a function of frequency is called absorption. [4]

Polar dielectrics that have more than one relaxation time do not satisfy Debye equation.

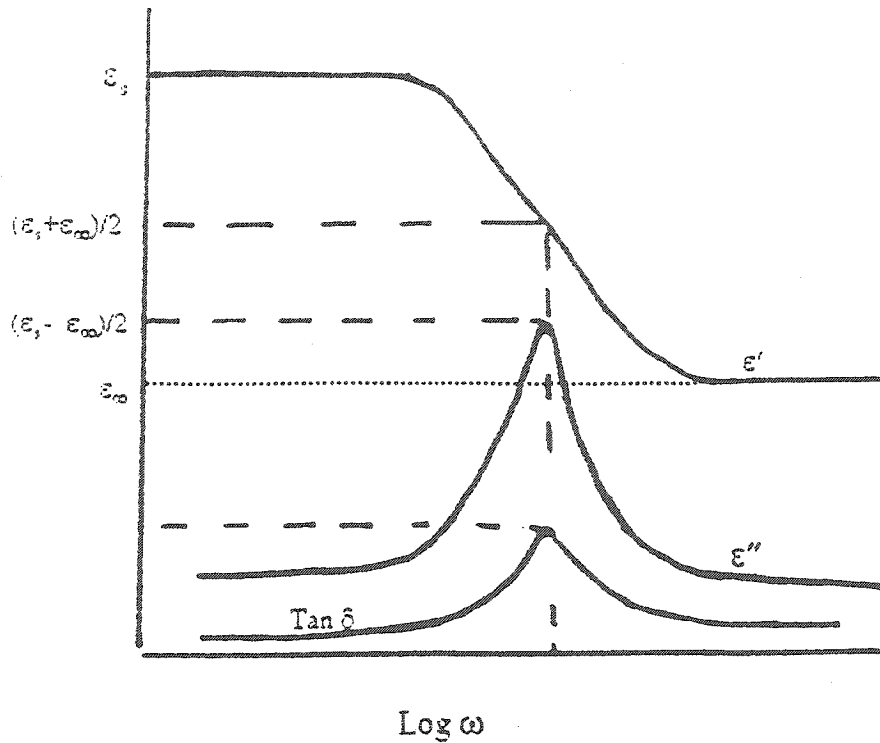


**Figure (1.4) Schematic Representation of Debye Equations Plotted as a Function of Frequency [1]**

There are other equations to describe relaxation phenomenon in some materials.

### 1.5 COLE - COLE RELAXATION [15]

$$\epsilon^* = \epsilon_\infty + \frac{(\epsilon_s - \epsilon_\infty)}{1 + [j\omega\tau_{cc}]^{1-\alpha}} ; \quad 0 \leq \alpha \leq 1 \quad [1.12]$$

$\alpha = 0$  for Debye relaxation.

Where  $\tau_{cc}$  is the mean relaxation time and  $\alpha$  is a constant for a given material.

A plot of equation [1.12] is shown in figure (1.5.1) and (1.5.2) for various values of  $\alpha$ .

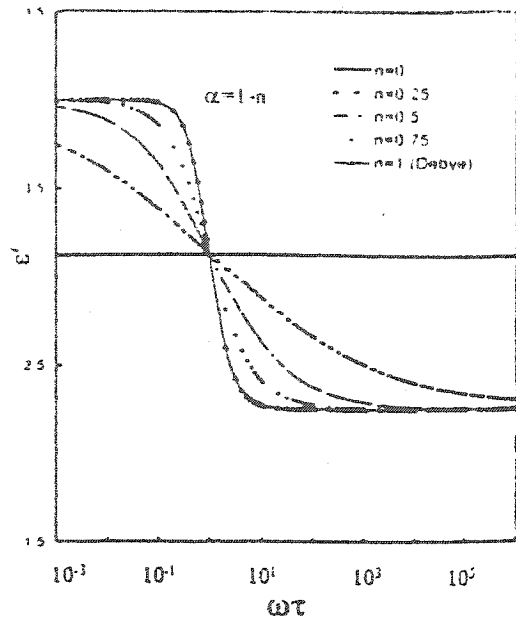


**Figure (1.5.1)**  
**Real part of  $\epsilon'$  in a Polar Dielectric**  
**According to Cole-Cole**

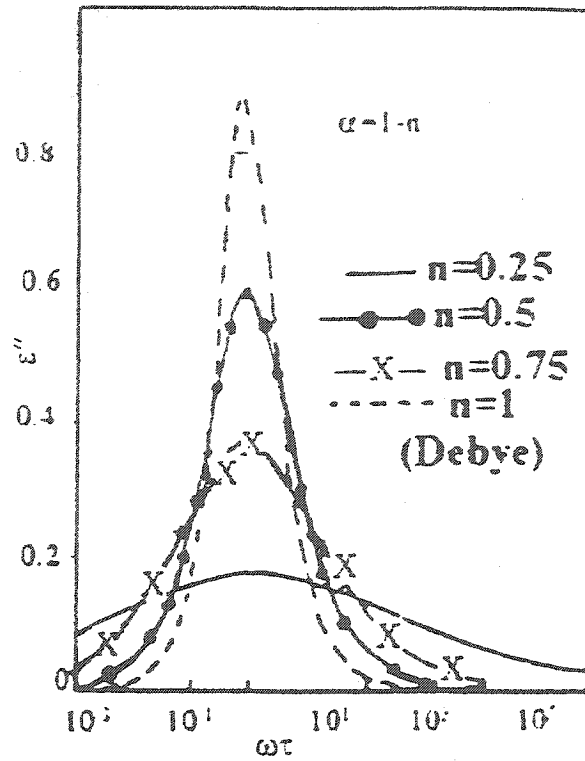


**Figure (1.5.2)**  
**Imaginary part of  $\epsilon'$  in a Polar**  
**Dielectric according to Cole-Cole**

### 1.6 DAVIDSON-COLE EQUATION [48]

Davidson-Cole have suggested the empirical equation

$$\epsilon^* = \epsilon_\infty + \frac{\epsilon_s - \epsilon_\infty}{[1 + j\omega\tau_{d-c}]^\beta} \quad [1.13]$$

Where  $0 \leq \beta \leq 1$  is a constant characteristic of the material.

### 1.7 HAVRILIAK AND NEGAMI DISPERSION [46]

H-N proposed a function for the complex Dielectric constant as

$$\frac{(\epsilon^* - \epsilon_\infty)}{(\epsilon_s - \epsilon_\infty)} = [1 + (j\omega\tau_{H-N})^{1-\alpha}]^\beta \quad [1.14]$$

## 1.8 KRAMERS - KRONIG RELATION

The complex nature of some physical parameters is such that their frequency dependent real and imaginary components cannot be specified independently from each other [4].

This is the case for the complex dielectric permittivity  $\varepsilon^*(\omega) = \varepsilon'(\omega) + j\varepsilon''(\omega)$

Where the Kramers-Kronig relations provide coupling between real and imaginary components. [5] [6]

As

$$\varepsilon'(\omega) = \varepsilon_{\infty} + \frac{1}{\pi} \int_{-\infty}^{\infty} \frac{\varepsilon''(\omega') d\omega'}{(\omega' - \omega)} \quad [1.15]$$

$$\varepsilon''(\omega) = -\frac{1}{\pi} \int_{-\infty}^{\infty} \frac{\varepsilon'(\omega') - \varepsilon_{\infty} d\omega'}{(\omega' - \omega)} \quad [1.16]$$

Integration can be carried out using an auxiliary variable  $\omega'$ , which is real.

The Kramers-Kronig relations have been used to derive  $\varepsilon'$  from  $\varepsilon''$  and compared with measured  $\varepsilon'$  as a means of verifying assumed  $\varepsilon'' - \omega$  relationship or vice versa.

The mathematical technique used by the Kramers-Kronig relations which allows the one component to be defined in terms of the other is the Hilbert transform since  $\varepsilon'(\omega)$  and  $\varepsilon''(\omega)$  can be shown to be Hilbert transform pairs.

The practical formation of this Hilbert transform pair is not an easy task in most instances. We cannot produce an analytic function. In this thesis numerical methods and their application to experimental results are successfully demonstrated.



## CHAPTER 2

# NUMERICAL COMPUTATION OF THE DIELECTRIC PERMITIVITY

### 2.1 FOURIER TRANSFORM

The Fourier transform (FT) of a waveform  $\omega(t)$  is

$$W(f) = F[\omega(t)] = \int_{-\infty}^{\infty} [\omega(t)e^{-2j\pi ft}] dt \quad [2.1]$$

### 2.2 SYMMETRY PROPERTIES OF FOURIER TRANSFORM APPLICABLE IN THIS STUDY

If a periodic function is symmetrical about the vertical axis the corresponding Fourier components contain only cosine terms, where as if it is antisymmetrical about the vertical axis the series contain sine terms only [33].

It is useful to define the following.

- (a) A function  $f(t)$  has an even symmetry of  $t$  if

$$f(t) = f(-t)$$

- (b) A function  $f(t)$  has odd symmetry of  $t$  if

$$f(t) = -f(-t)$$

### 2.3 CONVOLUTION OPERATION (\*)

The convolution of a waveform  $\omega_1(t)$  with a waveform  $\omega_2(t)$  produces a third waveform  $\omega_3(t)$  according to the operation

$$\omega_3(t) = \omega_1(t) * \omega_2(t) = \int_{-\infty}^{\infty} \omega_1(\lambda) \cdot \omega_2(t - \lambda) d\lambda \quad [2.2]$$

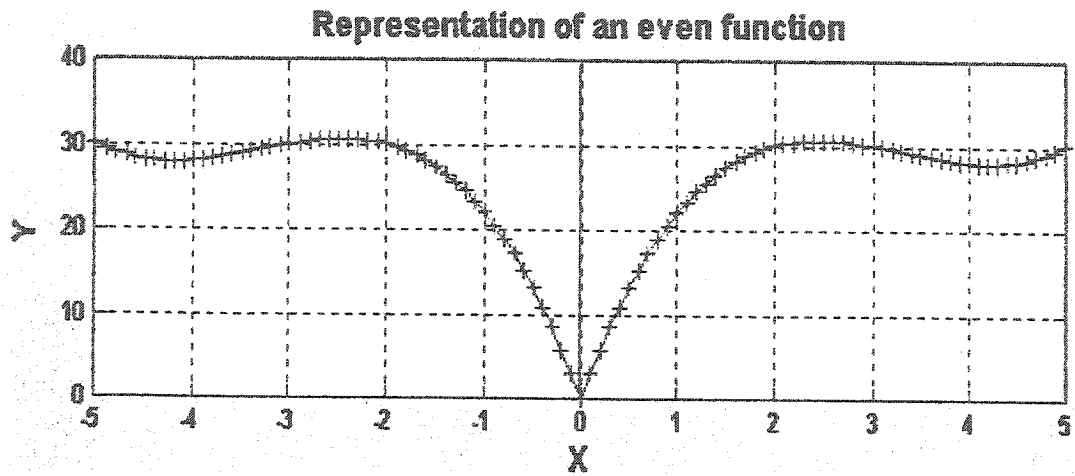


Figure (2.1)

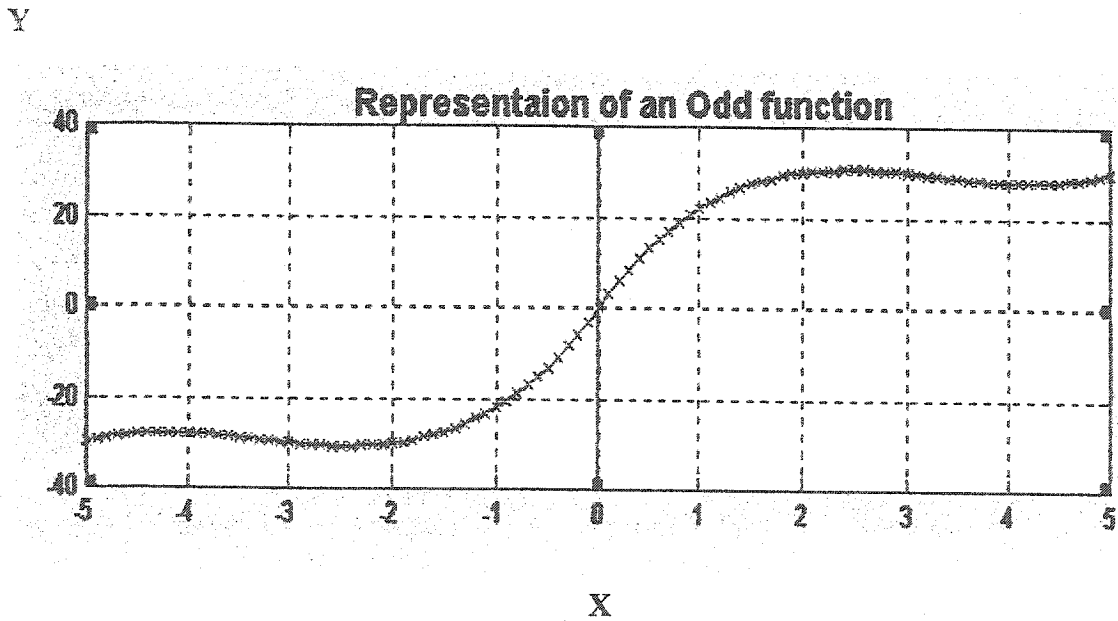


Figure (2.2)

## 2.4 HILBERT TRANSFORM

$$\text{Hilbert transform of } x(t) \text{ is denoted by } \hat{x}(t) = x(t) * \frac{1}{\pi t} = \frac{1}{\pi} \int_{-\infty}^{\infty} \frac{x(\lambda)}{(t-\lambda)} d\lambda \quad [2.3]$$

\* Denotes the convolution operation.

## 2.5 PROOF OF : $\varepsilon'(\omega)$ AND $\varepsilon''(\omega)$ ARE INDEED HILBERT TRANSFORMS OF EACH OTHER.

The Kramer-Kronig relations are

$$\varepsilon'(\omega) = \varepsilon_{\infty} + \frac{1}{\pi} \int_{-\infty}^{\infty} \frac{\varepsilon''(\omega') d\omega'}{(\omega' - \omega)} \quad [2.4]$$

and

$$\varepsilon''(\omega) = -\frac{1}{\pi} \int_{-\infty}^{\infty} \frac{[\varepsilon'(\omega') - \varepsilon_{\infty}] d\omega'}{(\omega' - \omega)} \quad [2.5]$$

Taking Hilbert transform of equations [2.5]

$$\begin{aligned} \hat{\varepsilon}'' &= \varepsilon''(\omega) * \frac{1}{\pi\omega} \\ &= \int_{-\infty}^{\infty} \varepsilon''(\omega') \left[ \frac{1}{\pi(\omega - \omega')} \right] d\omega' \end{aligned}$$

Rewriting,

$$\hat{\varepsilon}''(\omega) = \frac{1}{\pi} \int_{-\infty}^{\infty} \frac{\varepsilon''(\omega') d\omega'}{(\omega - \omega')} \quad [2.6]$$

$$\text{or, } \hat{\varepsilon}''(\omega) = -\frac{1}{\pi} \int_{-\infty}^{\infty} \frac{\varepsilon''(\omega') d\omega'}{(\omega' - \omega)} \quad [2.7]$$

Substituting equation (2.7) in (2.4),

$$\text{We have, } \hat{\varepsilon}''(\omega) = \varepsilon_{\infty} - \varepsilon'(\omega) \quad [2.8]$$

Similarly, since the Hilbert transform of a constant is zero

We have,

$$\hat{\varepsilon}'(\omega) = \varepsilon''(\omega) \quad [2.9]$$

The Hilbert transform may be implemented in the frequency domain by direct computation of

$$\varepsilon'(\omega) = \left[ \frac{1}{\pi\omega} \right] * \varepsilon'(\omega) \quad [2.10]$$

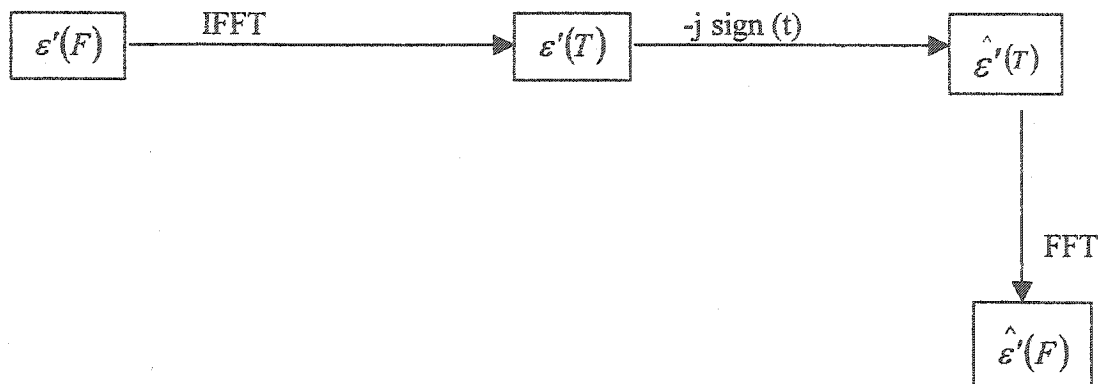
For discrete samples this becomes a matrix multiplication. Computation of this formula is very much time consuming since it requires  $n^2$  multiplications and additions. Such a computational burden can greatly be reduced by transforming the data into time domain by taking inverse Fourier transform. Then convolution operation in one domain becomes multiplication in the other domain [33].

These transformed data are next multiplied by,

$$-j \operatorname{sign}(t) \quad \begin{cases} -j = \text{for } t > 0 \\ j = \text{for } t < 0 \end{cases} \quad [2.11]$$

Finally these data are transformed back to the original frequency domain by taking Fourier transform.

## 2.6 THE FLOW CHART OF THE OPERATION.



In the present thesis the above method was used to obtain through Hilbert transform, one component of the dielectric constant from the other.

In a practical measurement,  $\varepsilon'(f)$  is measured at evenly spaced intervals,  $\Delta f$  (Hz) and initial frequency to a frequency  $f_{\infty}$ (Hz);

The latter being the frequency where  $\varepsilon_{\infty}$  is deemed to have been reached the minimum. Also the start frequency must be equal to or be a multiple of the incremental frequency. The technique also requires data at zero Hz and so it is necessary to either make a measurement at DC or to assume that the zero frequency data are the same as those obtained at the first measurement point.

Further more since the FFT technique requires the signal to be transformed to be periodic the negative of  $\varepsilon'(f)$  from 0 to  $-f_{\infty}$ (Hz) must be generated.

This is a simple matter since  $\varepsilon'(f)$  is an even function of  $f$  and is easily implement in software.

## 2.7 APPLICATION OF HILBERT TRANSFORM TECHNIQUE

To test the accuracy of the proposed technique it was first applied to theoretical Debye curves where one knows what the resultant Hilbert transform should be. It is then tested on data obtained in a dynamic situation.

Initially Debye equation [1.9] with  $\varepsilon_{\infty=0}$  was plotted for 8192 sample points and the resultant plots of  $\varepsilon''(\omega)$ ,  $\varepsilon'(\omega)$  and its Hilbert transform  $\hat{\varepsilon}'(\omega)$  were obtained. Then it is tested again for 16384 sample points. Thus having shown the technique to be successful for theoretically generated data, it is then applied to experimental data obtained for semi crystalline polychlorotrifluoroethylene (PCTFE) and Nomex<sup>TM</sup> 410.

## 2.8 NUMERICAL COMPUTATION OF FOURIER TRANSFORMS

With the convenience of personal computers and the availability of digital signal processing algorithms the spectrum of a wave form can be easily approximated by using the discrete Fourier transform (DFT). Here we show how the DFT can be used to compute samples of the continuous Fourier transform (CFT) of equation. [33]

The discrete Fourier transform (DFT) is defined by,

$$X_{(n)} = \sum_{K=0}^{K=N-1} x(k) e^{-j[2\pi/N]NK} \quad [2.12]$$

Where  $k=0, 1, 2, 3, \dots, N-1$

N is the number of samples

Equations [2.7] and [2.12] are definitions implemented on a digital computer to N values for the DFT and IDFT respectively.

The MATLAB uses the DFT and IDFT definitions that are given by equation [2.12] except that the elements of the vector are indexed 1 through N instead of 0 through N-1.

Thus the Matlab FFT algorithms are related to equation [2.12] by

$$X = \text{fft}(x)$$

$$x = \text{ifft}(X)$$

Where x is an N element vector corresponding to samples of the waveform and A is the N element DFT vector.

N is chosen to be a power of 2.

$N = 2^m$  Where m is a positive integer.

## 2.9 DFT TO COMPUTE THE CONTINUOUS FOURIER TRANSFORM

The relationship between the discrete Fourier transform and the continuous Fourier transform will now be examined. It involves three concepts.

Windowing, sampling and periodic sample generation.

Suppose that the Continuous Fourier Transform of a wave  $\omega(t)$  is to be evaluated by use of the Discrete Fourier Transform. The waveform is first windowed (truncated) over the interval  $(0, T)$ . So that only a finite number of samples  $N$  are needed.

The windowed waveform denoted by the subscript  $w$  is

$$W_w(t) = \begin{cases} \omega(t) & 0 \leq t \leq T \\ 0 & \text{elsewhere} \end{cases} \quad [2.13]$$

The Fourier transform of the windowed wave is

$$W_w(f) = \int_{-\infty}^{\infty} W_w(t) e^{-j2\pi ft} dt \quad [2.14]$$

$$= \int_0^T \omega(t) e^{-j2\pi ft} dt \quad [2.15]$$

Now we approximate the CFT using a finite series to represent the integral

Where,  $t = k\Delta t$   $f = n/T$   $dt = \Delta t$  and  $\Delta t = T/N$

## 2.10 IMPLEMENTATION PROCEDURE

### Step (1)

In a practical measurement  $\varepsilon'(f)$  has to be measured at evenly spaced intervals from a start frequency of  $\Delta f$  (Hz) to  $f_{\infty}$  (Hz): the latter being the frequency where  $\varepsilon_{\infty}$  is deemed to have been reached.

### Step (2)

$\varepsilon'(f)$  at  $f = 0$  must be used (d.c.value) or obtain by extrapolation of the curve.

### Step (3)

Since the FFT technique needs the signal to be transformed to be periodic using symmetry property the negative of  $\varepsilon'(f)$  from  $-f_{\infty}$  to 0 must be generated.

[Thus period of signal is  $\varepsilon'(f)$  has an even symmetry and  $\varepsilon''(f)$  has a selected odd symmetry.]

### Step (4)

Inverse Fourier transform.

### Step (5)

Hilbert transform.

### Step (6)

Fourier transform.



## CHAPTER 3

### LABORATORY MEASUREMENT

#### 3.1 MEASUREMENT OF DIELECTRIC PROPERTIES

Brief introduction is given about the measurement of complex permittivity and introduction about the instruments that were used in the measurement methodology.

#### 3.2 AVAILABLE METHODS FOR MEASUREMENT OF DIELECTRIC PROPERTIES

The dielectric properties of materials have been shown be very dependent on the frequency of their measurement. No one-measurement technique is available, however, that will give the entire frequency range is needed to characterize the entire spectrum. Several techniques are therefore used, each useful only in a certain frequency range [29].

A summary of these methods are shown in Table 4.1 [29]

**Table 3.1 – EXPERIMENTAL METHODS FOR THE MEASUREMENT OF DIELECTRIC PROPERTIES**

Frequency Range	(Hz) Methods
$10^{-4}$ to $10^{-1}$	D.C. Transient Measurements
$10^{-2}$ to $10^2$	Ultra Low Frequency Bridge
10 to $10^7$	Schering Bridge and Auto Balancing Bridge
$10^5$ to $10^8$	Resonance Circuits
$10^8$ to $10^9$	Coaxial Line and Re-entrant Cavity
$10^9$ to $3 * 10^{10}$	$H_{01n}$ Cavity Resonator and Wave guides

The methods shown in Table 3.1 can generally be divided into two groups. Those less than  $10^8$  Hz are referred to as lumped circuit methods, while those greater than  $10^8$  Hz are called distributed circuit methods. The lumped circuit methods are designed to measure a cell capacitance and resistance, which can be related to the dielectric properties of the sample. In contrast distributed circuits are designed to measure an attention factor,  $\alpha$  and a phase factor  $\beta$ , which are also be related to dielectric properties.

### 3.3 DIELECTRIC PROPERTY MEASUREMENT PRINCIPLE

It has been shown in the previous section that the dielectric properties of a material can be measured in several ways. However, often the nature of the materials to be measured, the application, the desired precision and the equipment costs severely limit the experimental approaches. Using Keithley LCZ 3330 and HP-4275A Impedance/Gain phase Analyser, the frequency dependent capacitance and resistance of the capacitor containing the desired sample could be monitored and related to the dielectric properties of the sample.

The Keithley model LCZ 3330 has frequency range from 40 Hz to 100 KHz, while HP-4275A was chosen because of its wide frequency range (10KHz-10MHz) and low cost (relative to analysers in the microwave region). The use of the parallel plate capacitor allows for easy online measurement since the polymer films can be placed directly between the electrodes. This arrangement was further extended to varying temperature environment using “ Environmental Test Chamber”.

The dielectric sample placed in the capacitor can be considered electrically equivalent to a capacitance,  $C_x$  in parallel with a resistance,  $R_x$  figure 4.1 where  $C_x$  represents the samples ability to store charge and  $R_x$  represents its heat related loss.

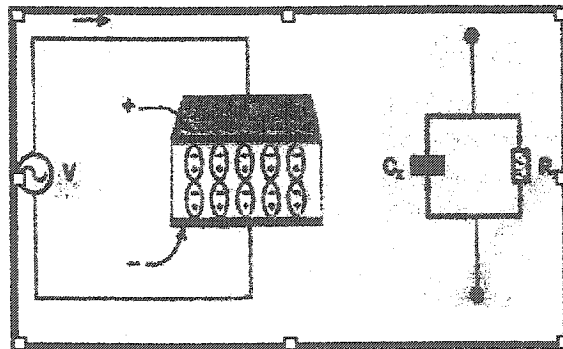


Figure 3.1A Parallel Plate Capacitor Containing a Dielectric Material and its Equivalent Circuit [29]

These values,  $C_x$  and  $R_x$  are measured using the impedance analyser and related to the dielectric properties of the sample as:

$$\varepsilon' = \frac{C_x}{C_0} \quad [3.1]$$

$$\varepsilon'' = \frac{1}{(R_x \omega C_0)} \quad [3.2]$$

$$\tan \delta = \frac{1}{(R_x C_x \omega)} \quad [3.3]$$

Where  $C_0$  is the cell capacitance in vacuum and is related to the electrode spacing and the electrode area through

$$C_0 = \frac{A \varepsilon_0}{d} \quad [3.4]$$

Where  $A$  is the electrode area,  $d$  is the electrode spacing and  $\varepsilon_0$  is the permittivity in vacuum given as  $8.8 \times 10^{-12}$  F/m [28]

### 3.4 ELECTRODES ARRANGEMENT

The research conducted required the measurement of both aramid paper and polymer films, with the facility to measure dielectric constant and loss factor. Two separate test cells were found to be required. To prevent erroneous results caused by fringing effects, figure 3.2, each cell used a three-terminal arrangement [29] in which guard electrode was used to prevent the unwanted fringing effects, figure 3.3. This arrangement reduces the errors tremendously and leads to the accurate result measurements for proper designing of insulation system

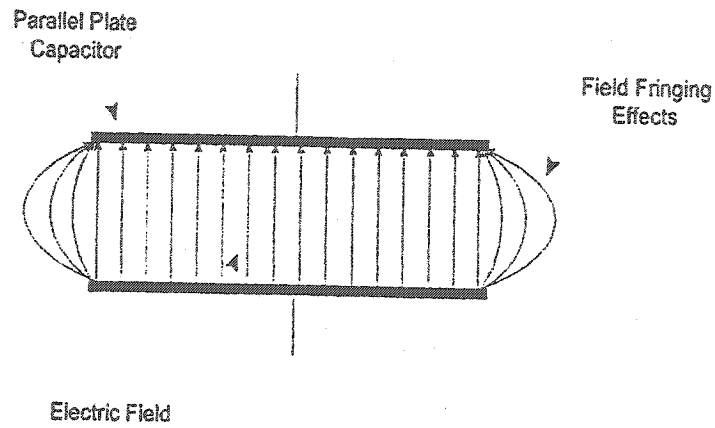


**Figure 3.2 Schematic Representation of Electric Fringing Effect of an Unguarded Parallel Plate Capacitor**

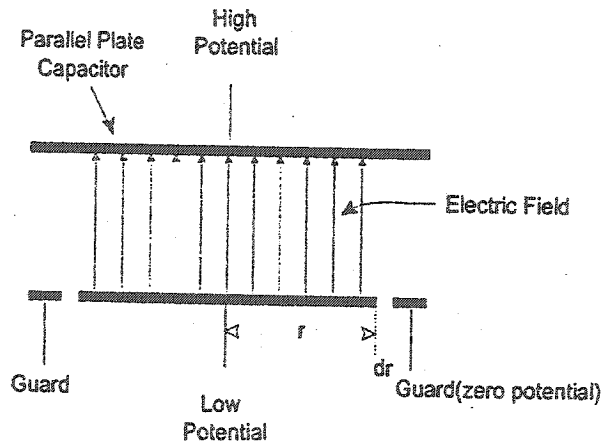


**Figure 3.3 Three Terminal Electrode Arrangement [29]**

Using this arrangement an effective electrode area,  $A_e$  must be used in equation (4.4). The effective area accounts for the gap between the low electrode and the guard ring can be expressed as:

$$A_e = \pi \left( r + \frac{dr}{2} \right)^2 \quad [3.5]$$

Where  $r$  is the radius of the inner ring

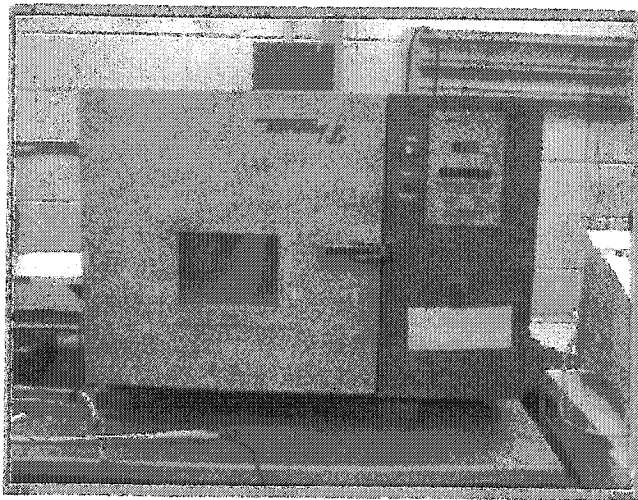
$dr$  is the difference of radius between guard ring and inner ring

### 3.5 EXPERIMENTAL APPARATUS USED FOR DIELECTRIC PROPERTIES MEASUREMENTS

The experimental arrangement consists of:

- a. Tenney Jr. Environment test chamber
- b. Keithely 3330 LCZ meter
- c. HP-4275A Multifrequency LCR meter
- d. Voltage/ Current Recorder

#### 3.5.1 ENVIRONMENTAL TEST CHAMBER



The Tenney Jr. temperature bench top test chamber offers outstanding performance, reliability and long life. It is a popular environmental chamber and is especially adaptable for laboratory use in product development, quality assurance, research electronic and MIL-STD testing. It is completely self contained and ready for immediate plug-in use.

The unit utilizes a dual compressor cascade mechanical refrigeration system. Sequential starting of compressor reduces starting current. Thus the system requires no CO<sub>2</sub> and is therefore free of the inconvenience and expense of this method. At the same time, the

Tenney Jr. can achieve a temperature that is 280 K colder than that possible with CO<sub>2</sub>, i.e. 193 K. Table 4.2 shows some features of Tenney Jr. Environmental chamber, while figure 4.4 shows some features of Tenney Jr. Environmental chamber, while figure 4.4 shows its front view. [34].

**Table 3.2 – SPECIFICATIONS OF TENNEY JR. ENVIRONMENTAL TEST CHAMBER**

Unit utilizes a dual compressor cascade mechanical refrigeration

Temperature Range:	Degree centigrade	-80° C to 200° C
Interior Dimensions:	Inches	16" (W) × 21"(H) × 11"(D)
Heating Rate:	From 25°C to +200°C	55 minutes
Cooling Rate:	From +25°C to -80°C	65 minutes
Approximate Weight:	Pounds	200
Heating capacity:	Watt	500
Temperature Controller	-	TENNY-JRCO-0001

### 3.5.2 KEITHELY MODEL LCZ 3330 METER

The model 3330 LCZ meter is a high-accuracy full function LCZ meter, figure 4.5. The model 330 drives the device under test (DUT) with a sine wave signal. Impedance is determined by applying a know voltage, precisely measuring the resulting current that flows through the DUT and then computing the impedance magnitude and phase. Displayed parameters such as inductance, capacitance and resistance are calculated from the magnitude and phase of the computed impedance. Table 4.3 below shows some features and specifications of 3330 meter [34]

The model 3330 LCZ meter is a high-accuracy full function LCZ meter, figure 3.5. The model 330 drives the device under test (DUT) with a sine wave signal. Impedance is determined by applying a known voltage, precisely measuring the resulting current that flows through the DUT and then computing the impedance magnitude and phase. Displayed parameters such as inductance, capacitance and resistance are calculated from the magnitude and phase of the computed impedance. Table 3.3 below shows some features and specifications of 3330 meter [41]

**Table-3.3- SPECIFICATIONS OF KEITHLEY MODEL LCZ 3330 METER [41]**

Model has two displays:	
Measurement functions are:	(L,C,R,/Z/ $\theta$ ,D,ESR,G,X,Q,V,I)
Measurement frequency range:	940 Hz to 100 KHz)
Measurement signal level:	(10m Vrms to 1.1 Vrms)
GPIB (IEEE-488):	Interface for Computer control
Measuring times:	Slow (480 msec)

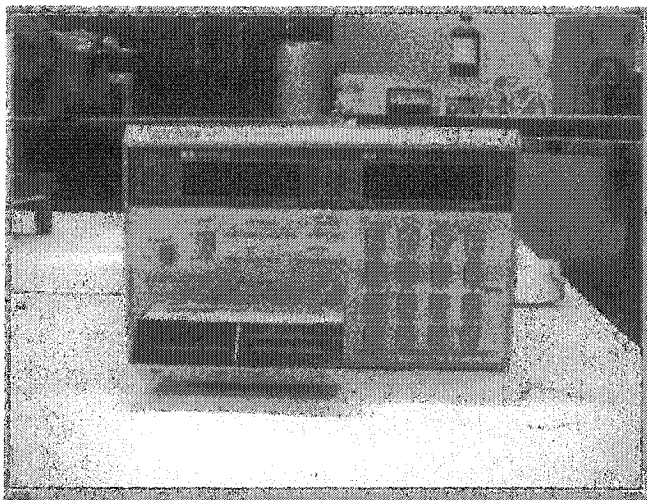


**Figure 3.4 Front view of Keithley Model LCZ 3330 Meter [29]**

### 3.5.3 MULTI-FREQUENCY HP-4275 (LCR) METER

The HP model 4275 multi-frequency LCR meter is a high performance, fully automatic test instrument designed to measure the various component measurement parameter values of an impedance element in the relatively high frequency region. Complete specifications of model 4275A multi-frequency LCR meter are given in table 3.4. These specifications are the performance standards or limits against which the instrument is tested. Measured values are displayed by the two-4-1/2 digit numeric displays along with appropriate units. A high resolution-operating mode provides 5-1/2 digit resolution plus lesser significant data by averaging the measured values every ten measurements.

**Table-3.4 – SPECIFICATIONS OF HP-4275A MULTI-FREQUENCY LCR METER [51]**

Parameter Measured:	(C,L,/Z/,D,Q,ESR,G,X,B, $\theta$ )
Measurement Circuit Modes:	(Auto, Series and Parallel)
Measurement frequencies:	(10KHz, 100KHz, 200KHz, 400KHz, 1MHz, 2MHz, 4MHz and 10MHz)
HP-IB connector	Used for the inter-comm: with other HP-IB devices

### 3.6 EXPERIMENTAL SETUP FOR DIELECTRIC MEASUREMENTS

The complete experimental set up, figure 3.6, consisted of the designed test cells attached to a HP-4275A. Impedance/Gain analyser using coaxial wires and a HP-16047A test fixture. The high potential and low potential electrodes were connected to the HP-10647A test fixture, which in turn interfaced with the analyser, figure 4.6 where  $H_p$  is the high potential and  $H_c$  is the high current,  $L_p$  is the low potential and  $L_c$  is the low current. The guard ring electrode was connected to ground. A personal computer was used for data analysis.



## EXPERIMENTAL SET-UP

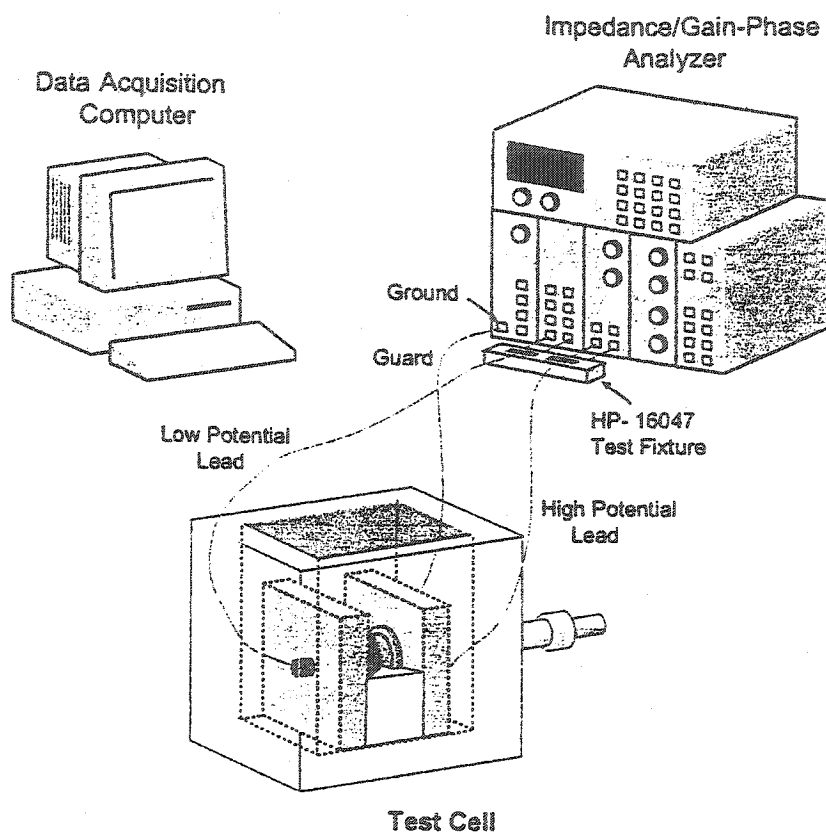


**Figure 3.6 A Schematic Diagram of the Experimental Set-up Consisting of a H-4275A Impedance/Gain -Phase Analyser, a Test Cell, and a Data Acquisition Computer**

The impedance,  $Z$ , is a complex and given as:

$$Z = R + jX = R_s + \left( \frac{R_x}{(1 + \omega^2 R_x^2 C_x^2)} \right) + j \left( \frac{\omega L - \omega^2 R_x C_x + \omega^2 R_x L C_x}{(1 + \omega^2 R_x^2 C_x^2)} \right) \quad [3.6]$$

Where  $R$  is the resistance and  $X$  is the reactance. Using this measurement the capacitance of the capacitor is calculated using the relationship [52]

$$C = \frac{1}{\omega X} \quad [3.7]$$

Where  $\omega$  is the test frequency. In addition the cell conductance,  $G$ , could also be calculated by:

$$G = \frac{1}{R} \quad [3.8]$$

The value of  $R_s$  and  $L$  (inductance) are parasitic values in the equivalent circuit due to the lead wires and the electrodes while  $C_x$  and  $R_x$  can be related to the charge storage and loss in the of the dielectric material in the capacitor respectively. To limit the parasitic effect the leads were kept as short as possible and shielded. As the measurement frequency is increased, however, the calculated circuit parameters. This inductance resonance effectively limited the measurement of the dielectric properties to 1 MHz. The accuracy of the analyser could be controlled to some extent by several measurement parameters. These parameters include the test frequency (due to the inductance effect) the number of measurements averaged, the integration time of the measurement and the applied voltage to the cell. [52]

## CHAPTER 4

### MEASUREMENT OF DIELECTRIC PROPERTIES AT LOW FREQUENCY

#### 4.1 MEASUREMENT OF CHARGING AND DISCHARGING CURRENTS TO OBTAIN DIELECTRIC PROPERTIES

It has been established that the charging/discharging currents can be used to obtain the low frequency dielectric loss ( $\varepsilon''$ ) and the dielectric relaxations, which occur in the low frequency range [42,43].

The discharging current decay is given by the equation  $\phi(t) = t^{-n}$

The complex dielectric constant of material is given by

$$\varepsilon^* = \varepsilon' - j\varepsilon'' \quad [4.1]$$

Where,  $\varepsilon^*$  is the complex dielectric constant

$\varepsilon'$  is the real part of the dielectric constant

$\varepsilon''$  is the dielectric loss factor.

The theoretical equation for  $\varepsilon'$  and  $\varepsilon''$  in terms of current produced by the application of a step voltage [42,43] are

$$\varepsilon'(\omega) = \frac{1}{C_a \left[ C_0 + \int \phi(t) \cos \omega t . dt \right]} \quad [4.2]$$

$$\varepsilon''(\omega) = \frac{1}{C_a \left[ \frac{G_0}{\omega} + \int_0^{\infty} \phi(t) \sin \omega t . dt \right]} \quad [4.3]$$

Where  $C_0$  is the capacitance of sample at high frequencies,

$C_a$  is the capacitance of sample if sample replaced by air

$G$  is steady state d.c. Conductance

$\omega$  is the angular frequency

$\phi(t)$  is the current following in the sample

After applying unit voltage at  $t=0$  and is called as the decay function of the dielectric

$\phi(t)$  does not include the steady state conduction current from which  $G_0$  is calculated and thus  $\phi(\infty) = 0$

$\phi(t)$  Can be approximated over a wide range of values by equation,

$$\phi(t) = \beta C_0 t^{-n} \quad [4.4]$$

Where  $\beta$  and  $n$  are constant for a material.

Substituting the value of  $\phi(t)$  in equations [4.2] and [4.3]

We get,

$$\varepsilon'(\omega) = \frac{C_0}{C_a \left[ 1 + \beta \omega^{n-1} \tau (1-n) \cos \left\{ \frac{(1-n)\pi}{2} \right\} \right]} \quad [4.5]$$

$$\varepsilon''(\omega) = \frac{1}{C_a \left[ \frac{G_0}{\omega} + \beta \omega^{n-1} \tau (1-n) \cos \left( \frac{n\pi}{2} \right) \right]} \quad [4.6]$$

The equation [4.4] holds good for  $0 < n < 1$  and equation [4.6] for  $0 < n < 2$ .

Hamon [23] expressed the charging current  $\phi(t_1)$  at a particular time  $t_1$  as

$$\varepsilon^n = \frac{[G_0 + \phi(t_1)]}{\omega C_a} \quad \text{and} \quad [4.7]$$

$$\omega t = \left[ \tau(1-n) \cos\left(\frac{n\pi}{2}\right) \right]^{-1/n} \quad [4.8]$$

The right side of the equation is almost independent of  $n$  in the range of  $0.3 < n < 1.2$  and taking a 3% accuracy the mean value can be taken as 0.63. To an approximate accuracy the above equation can now be written as

$$\varepsilon^n \approx \left\{ G_0 + \phi\left(\frac{0.63}{\omega}\right) \right\} \quad [4.9]$$

If  $I(t)$  is defined as the total charging current as a function of time after the application of the steep voltage  $v$ . i.e. the sum of the charging current and the conduction current and is expressed as,

$$i(t) = V [G_0 + \phi(t)] \quad [4.10]$$

and the equations can now be transformed to a

$$\varepsilon^n \approx \frac{I(0.63)}{\omega^2 C_a V} \quad [4.11]$$

Hamon [23] also provided a detailed analysis and showed that even if  $\phi(t)$  departs considerably from equation [3.4] the approximation holds well. The above has also been confirmed by Baird [24].

In addition to the restriction for the values of  $n$  the superposition principle must also hold good. The anomalous charging and the discharging currents are reversible and proportional to applied voltage. The charging current so often the discharging current is used in order to offset the affect of the conduction current contribution.

#### 4.2 EXPERIMENTAL MEASUREMENTS

The experimental arrangement for measurement of absorption currents is relatively simple and a typical set up is shown in fig (4.1). The transformation from the time domain to the frequency domain involves the assumption that the current is measured in the integral 0 to infinity, which is not attained in practice. The necessity to truncate the integrand at  $t > t_{\max}$  ceases to contribute to  $\epsilon'$  and  $\epsilon''$ . The lowest frequency at which  $\epsilon'$  and  $\epsilon''$  are evaluated depends on the longest duration of the measurement and the current magnitude at that instant.

Experimental set up for the study of charging and discharging currents

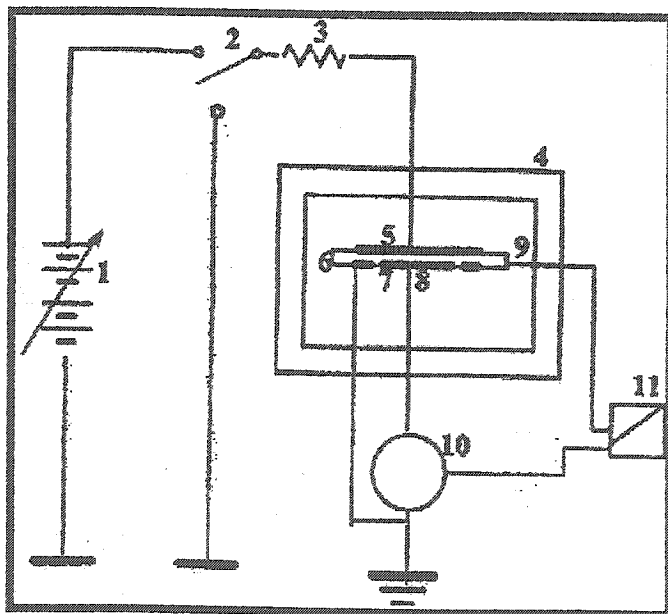


Figure (4.1)

1. **Brandburg Variable D.C Power Supply**
2. **Two Way Switch**
3. **Control Resister**
4. **Tenney Jr Environmental Chamber**
5. **High Voltage Electrode**
6. **Sample**
7. **Guard Ring**
8. **Measuring Electrode**
9. **Thermocouple**
10. **Keithley 617C Electrometer**
11. **Current Recorder**

#### **4.3 SAMPLE PREPARATION AND ELECTRODES:**

Before commencement of experiments, samples were heat treated for 12 hrs at 200°C to remove the moisture and improve the reproducibility of the results. Formation of the electrode is of paramount importance.

In laying down the conductive material the surface of the sample should not be chemically changed and care should be taken to avoid gaps between electrodes and the sample. The most efficient way of doing this is by the vacuum depositing of the electrodes on the sample. During the course of the experiments we have used conduction silver paint as electrode material.

The currents in the polyamide sample range from nano to pico amperes. ( $10^{-12}$ ). The measurement of such small currents is hampered by electrical noise. Making all wires as short as possible and fixing them securely to the ground minimized mechanical noise arising from the changes in system capacitance.

In order to minimize the low level spurious leakage currents a three terminal electrode system as shown in fig (4.2) [24] is used. This three terminal arrangement eliminates the fringing effect and improves the results tremendously.

### Three Terminal Electrode Assembly

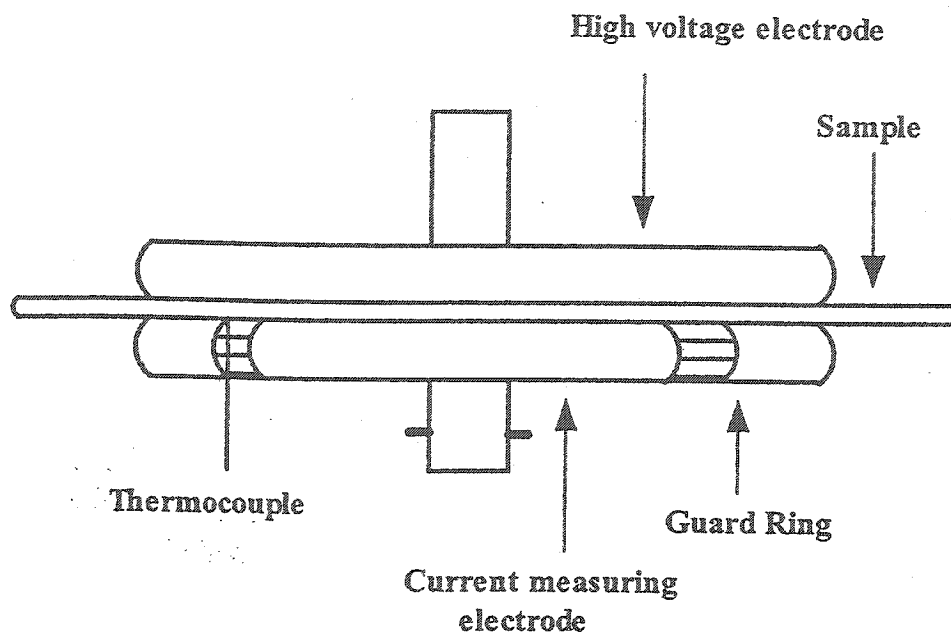


Figure 4.2



#### **4.4 APPARATUS USED FOR MEASUREMENT:**

The experimental arrangement consists of a high voltage direct current generator, Tenney junior environmental chamber, Keithley 617C electrometer and a voltage / current recorder.

An overview of the instrument specifications is given below.

##### **4.4.1 HIGH VOLTAGE D.C GENERATOR**

Brandenburg model 2307 was used for high voltage direct current generation. The voltage ranges from 0 to 5kV at 1mA.

##### **4.4.2 TENNEY JUNIOR ENVIRONMENTAL CHAMBER**

The Tenney junior environmental chamber is used to monitor and control temperature. It is accurate up to 0.1°C.

##### **4.4.3 KEITHLEY 617C ELECTROMETER**

The Keithley model 617C electrometer is a highly sensitive instrument designed to measure voltage current, charge and resistance.

The measuring range of model 617C is between 10mV to 200V for voltage measurements 0.1A to 20mA in the current mode. The very high input impedance and the extremely low input off set current allow accurate current measurement. It has a 5 digit display and a standard IEEE-488 interface along with a both preamp and 2V full along outputs on the rear panel.

It has an internal buffer that can store over 100 readings that are accessible from either the front panel or over the IEEE-488 bus.

## 4.5 EXPERIMENTAL PROCEDURE

The sample is pre-treated by increasing the temperature of environmental chamber up to 200°C and for 12 hrs to remove the moisture content. The procedure and thermal protocol adapted for the measurement of the charging / discharging current and conduction current is explained in sections below.

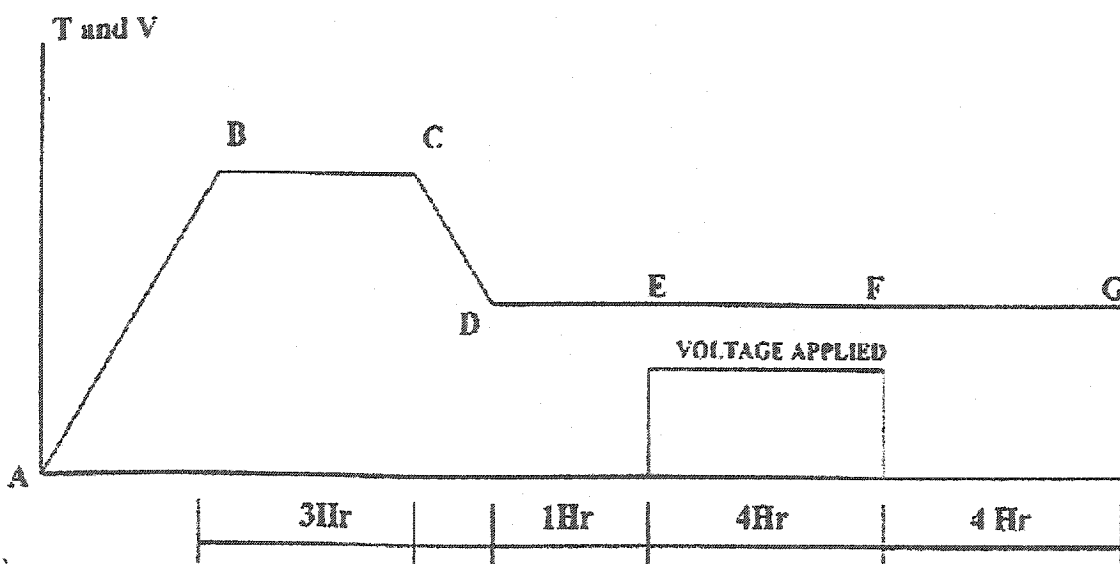


Figure 4.3

Thermal Protocol Adapted for Study of Charging and Discharging Currents

## 4.6 CHARGING / DISCHAGING CURRENT

Fig 4.1 shows the schematic arrangement of the study of the charging and discharging currents. After the preparation of the dielectric film, it is placed between two electrodes and kept in the environmental chamber. The currents are measured using a Keithley 617 c electrometer that is connected to the low voltage electrode and data acquisition system. The frequency of the sampling can be adjusted up to 4 KHz but most of the data are taken at 1 Hz. A thermocouple is also attached to the holder to monitor the temperature. The thermocouple is attached to the DT series board and voltage values are logged in the data files. Sawa [26] introduced thermal protocol and Govinda Raju [27] introduced a variation of this technique, which is adapted in this study. Fig 4.4 shows the thermal protocol that the dielectric material goes through during the course of the experiments. The thermal protocol consists of the following.

- A - B            Increase the environmental chamber temperature from the room to 200°C
- B - C            Hold the temperature constant at 200°C for 3 hours
- C - D            Lower the temperature to the desired value
- D - E - F        Maintain the desired temperature for 2 hours
- E - F            Apply the desired DC voltage for 4 hours and record the charging current
- F - G            Remove the DC voltage, short circuit the electrode for 4 hours and record the discharging currents.

The electrodes are short circuited through out the protocol, which starts at A and ends at E. Before each measurement a blank run was performed in order to free the sample from the extraneous charge. This run consisted of raising the temperature the sample at constant rate to 200°C with the electrodes short-circuited for a period of 6 hours.

## 4.7 LOW FREQUENCY DIELECTRIC LOSS FACTOR ( $\epsilon''$ )

The time dependence of discharging currents can be used to calculate the low frequency dielectric loss using Hamon approximation [23].

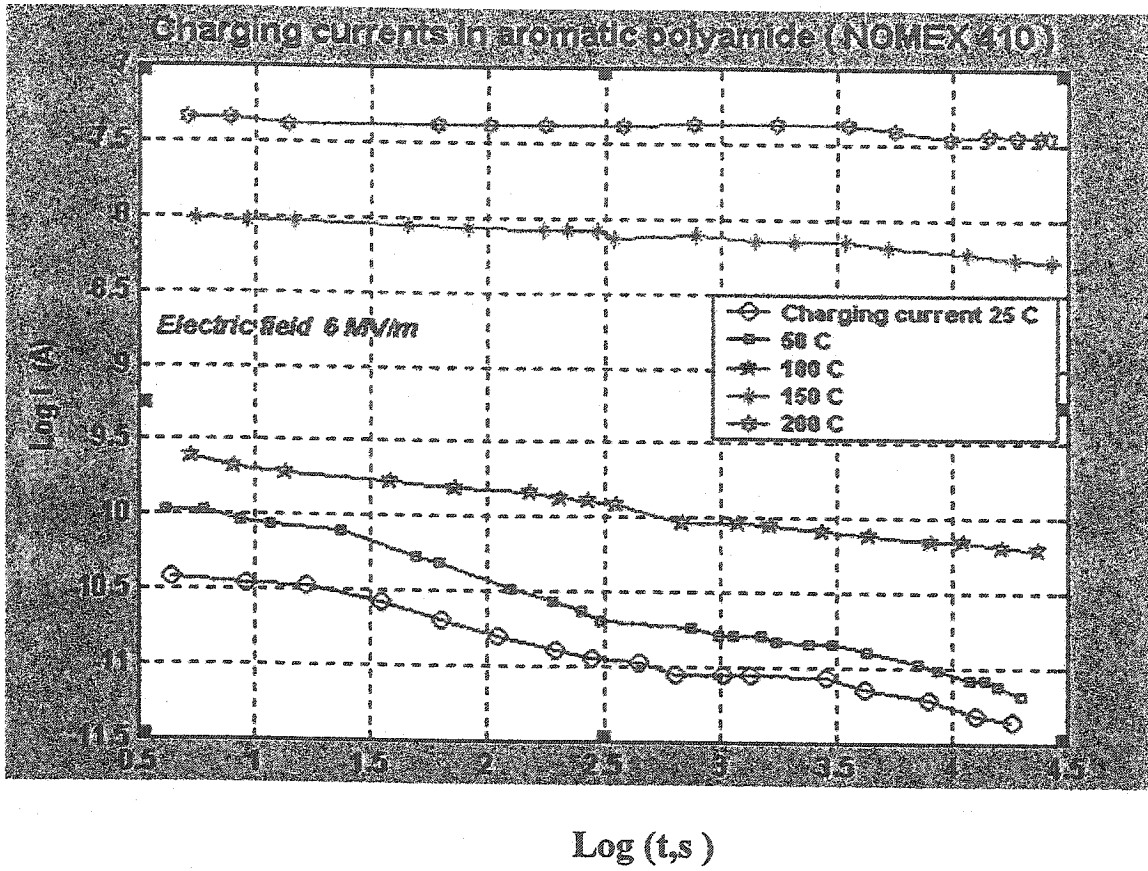


**Figure 4.4** Charging Currents in Aromatic polyamide (NOMEX 410)

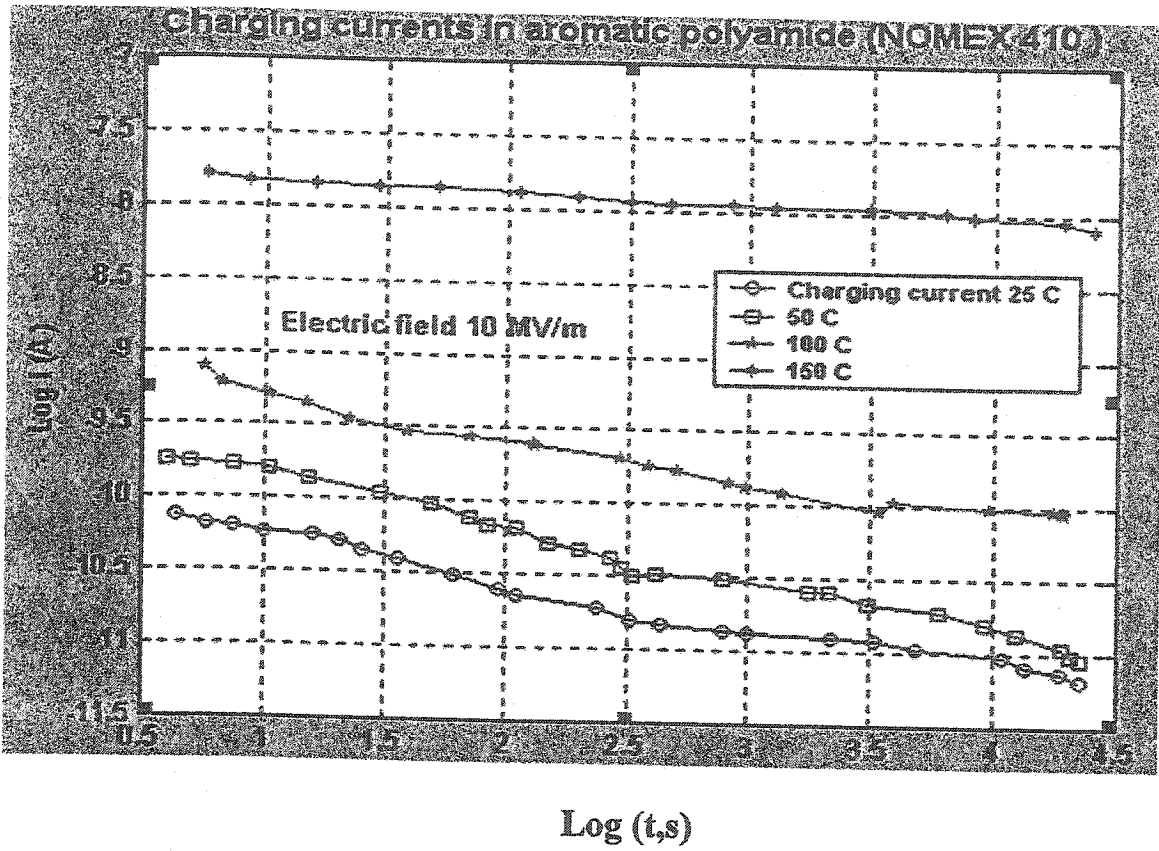


Figure 4.5 Charging Currents in Aromatic Polyamide (NOMEX 410)

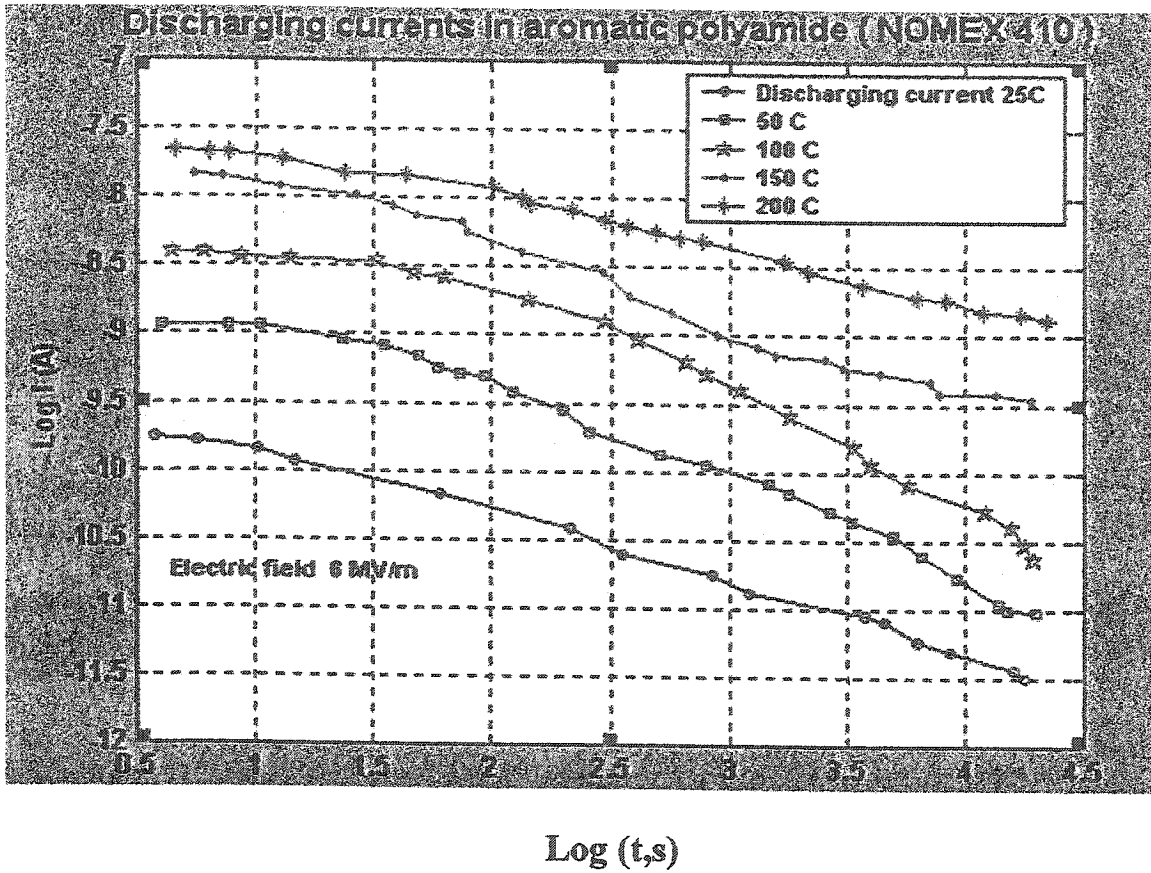


Figure 4.6 Discharging Currents in aromatic Polyamide (NOMEX 410)

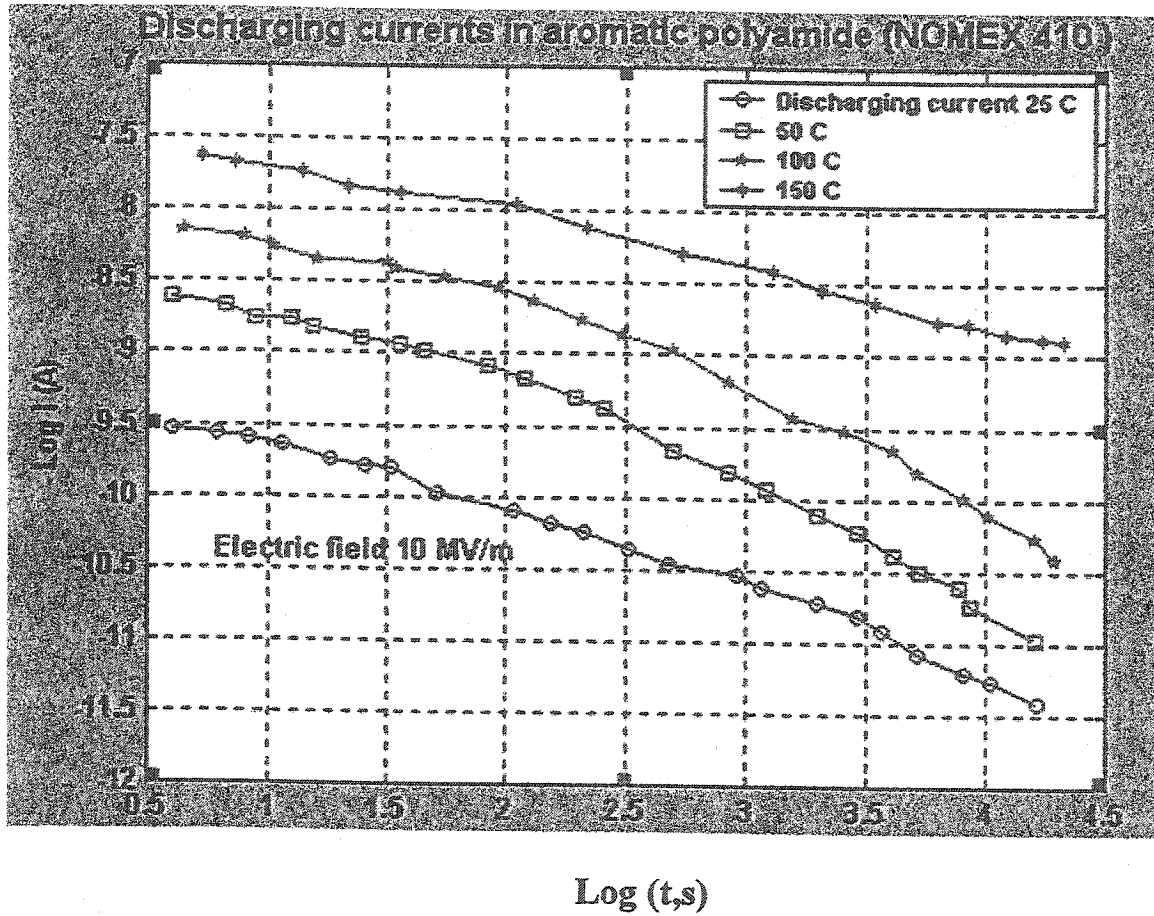


Figure 4.7 Discharging Currents in Aromatic Polyamide (NOMEX 410)

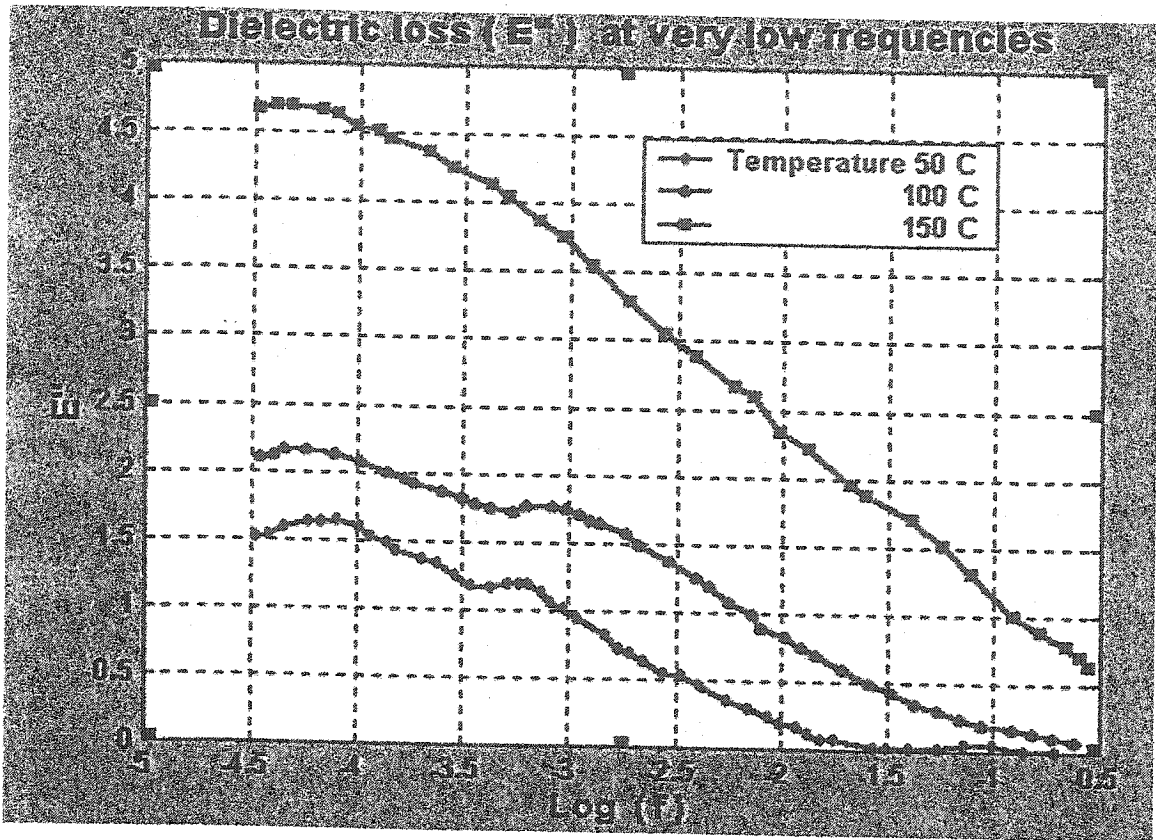


Figure 4.8 Dielectric Loss at Very Low Frequencies



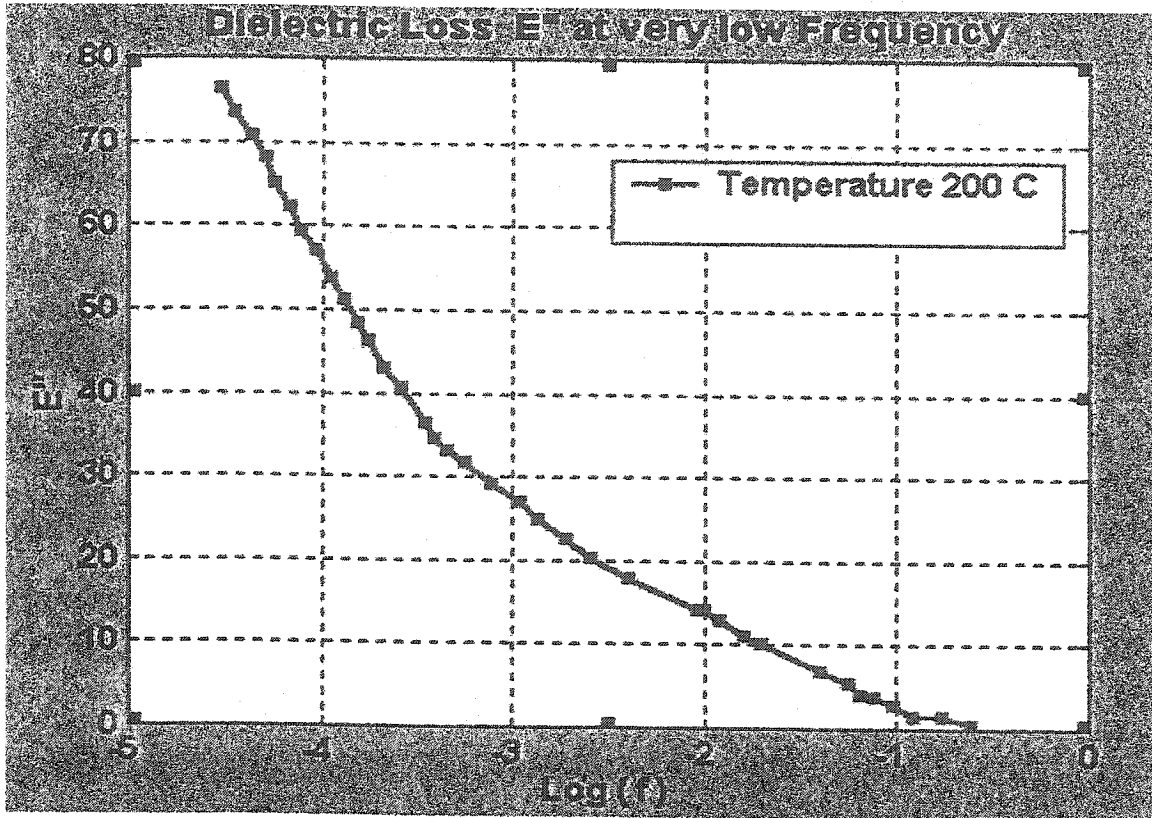


Figure 4.10 Dielectric Loss at very low Frequency

## CHAPTER 5

### INVESTIGATED DIELECTRIC MATERIALS

#### 5.1 INVESTIGATED DIELECTRIC MATERIALS AND THEIR ELECTRICAL PROPERTIES:

The purpose of this chapter is to give an overview of the dielectric materials studied.

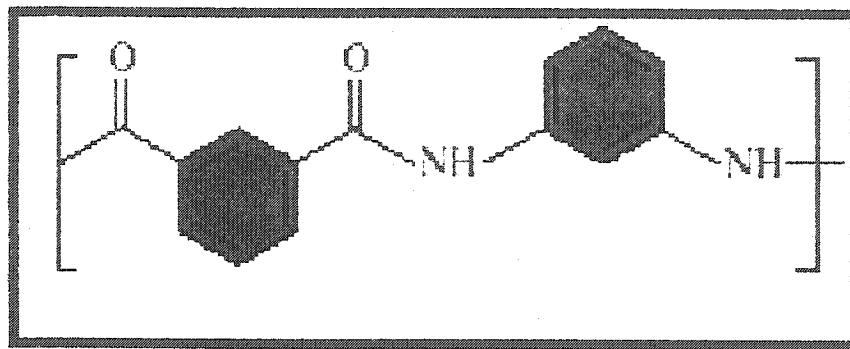


Figure 5.1 NOMEX Type 410

Nomex is a synthetic aromatic polyamide polymer that gives high level of electrical, chemical and mechanical integrity when converted into its various sheets forms. Used properly Nomex products can extend the life of electrical equipment reduce premature failures and repairs and act as a safeguard in unfrozen electrical stress situations.

Nomex products have characteristics, which make them ideally suited for electrical insulation applications. These characteristics may vary slightly in the different forms and types of Nomex.

A unique combination of properties gives Nomex superior characteristics

**(1) Inherent dielectric strength**

Withstands 450 – 1000V/mil depending on type and thickness.

**(2) Mechanical toughness**

Strong, resilient and thinner grades, flexible with good resistance to tearing and abrasion.

**(3) Thermal Stability**

Temperatures up to 200°C have little or no effect on the electrical or mechanical properties of Nomex.

**(4) Chemical Compatibility**

Essentially unaffected by solvents, resistant to acids and alkalis. Compatible with all classes of varnishes and adhesives, transformer fluids, lube oils and refrigerants.

Nondigestible not attacked by insects, fungi or moulds.

**(5) Moisture Insensitivity**

In equilibrium at 95% relative humidity Nomex papers maintain 90% of their bone-dry dielectric strength while many mechanical properties are actually improved.

**(6) Radiation Resistant**

Nomex is essentially unaffected by 800 megarads of ionising radiation.

**(7) Non-Toxic-flame Resistant**

Will not produce any known toxic reactions in human or animals or melt support combustion air.

## 5.2 APPLICATIONS

Because of its unique combination of excellent electrical, thermal and mechanical properties Nomex™ type 410-aramid papers has been widely adopted by the electrical industry for use in

### Motors and Generators:

Slot Cells	-	End laminates
Phase Insulation	-	Bushings
Wire Wrap	-	Pole pieces
Wedges	-	Mid – Sticks
Lend Insulation	-	V – rings

### Transformers

Wire Wrap	-	Lead Insulation
Core and Barrier Tubes	-	End pack out
Interphase	-	Layer

## 5.3 ELECTRICAL PROPERTIES

Important electrical properties of Nomex type 410 papers at room temperature and 50% relative humidity are shown in Table (5.1). The dielectric constant and dissipation factor to type 410 paper increase slightly with temperature up to 225°C (9430F). The dielectric strength is unaffected by temperature up to 225°C (430F) and maintains about 95% of its room temperature value at 250°C.

Table 5.1 TYPICAL ELECTRICAL PROPERTIES ARAMID PAPER

Nominal thickness(mil)	2	3	5	7	10	12	15	20	24	25.5	29	30
(mm)	.05	.08	.13	.18	.25	.30	.38	.51	.61	.65	.73	.76
Dielectric Strength												
-AC rapid rise												
(V/mil)	430	550	680	840	815	820	830	810	800	730	750	680
(kV/mm)	17	22	27	33	32	32	33	32	31	29	30	27
Full wave impulse												
(V/mil)	10 <sup>3</sup>	10 <sup>3</sup>	1400	1400	1600	N/A	1400	1400	N/A	N/A	N/A	1250
(kV/mm)	39	39	55	55	63	N/A	55	55	N/A	N/A	N/A	49
Dielectric constant at												
60 Hz	1.6	1.6	2.4	2.7	2.7	2.9	3.2	3.4	3.7	N/A	3.7	3.7
Dissipation factor												
60Hz ( $\times 10^{-3}$ )	4	5	6	6	6	7	7	7	7	N/A	7	7

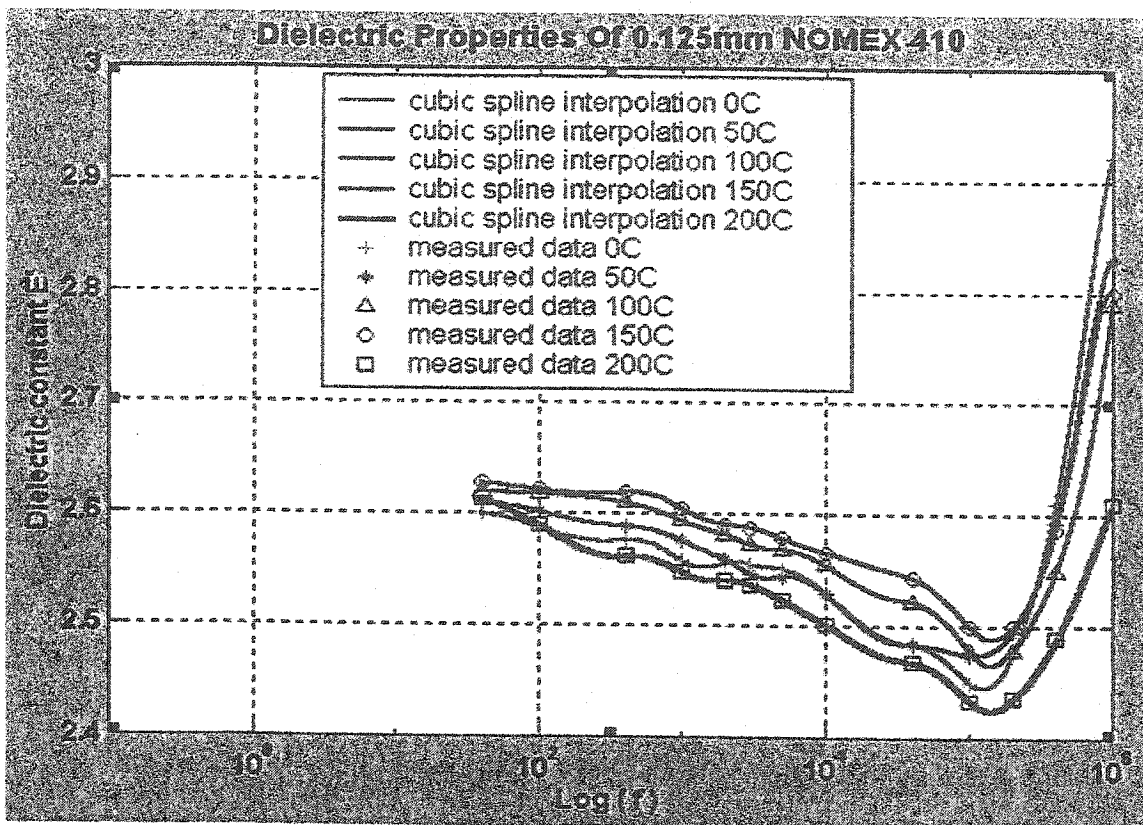


Figure 5.2 Dielectric Properties of 0.125mm NOMEX 410

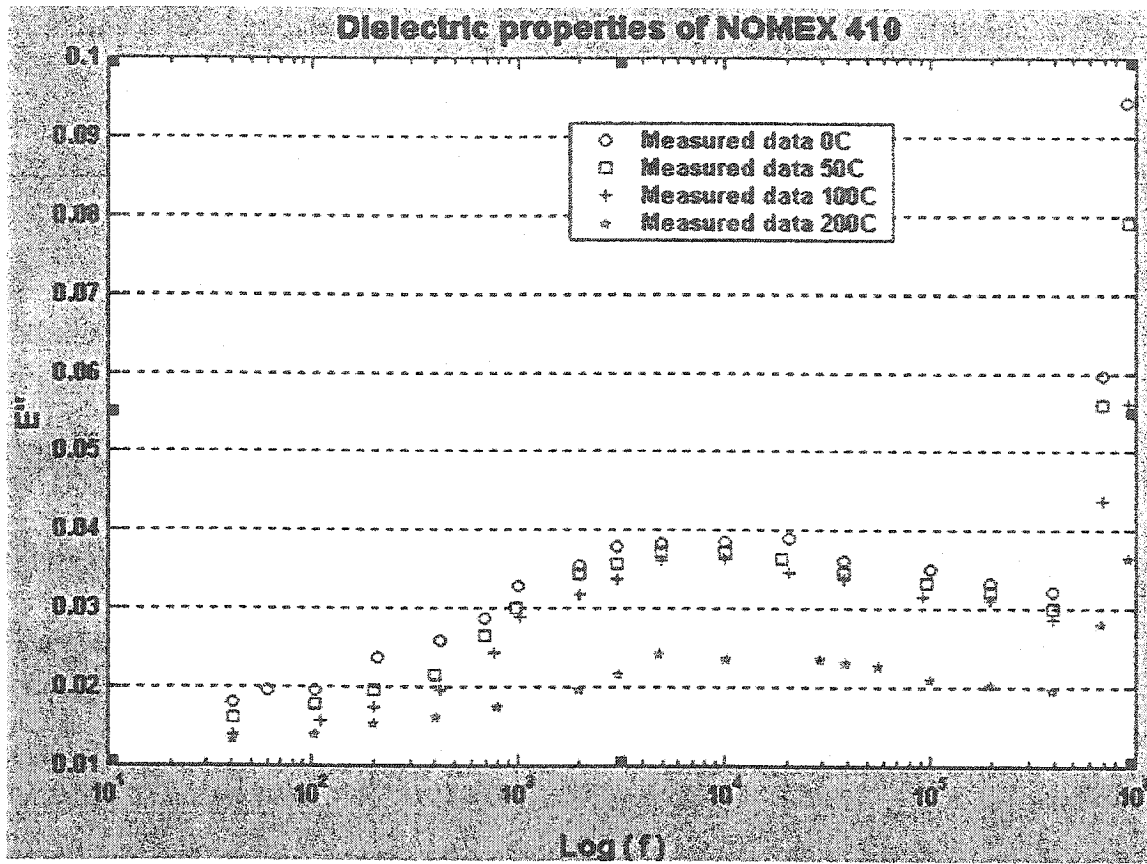


Figure 5.3 Dielectric Properties of NOMEX 410

## 5.4 SEMICRYSTALLINE POLYCHLOROTRIFLUOROETHYLENE (PCTFE)

### 5.4.1 CHEMICAL STRUCTURE

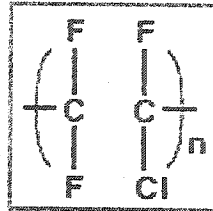


Figure 5.3.1 Atomic structure of PCTFE

PCTFE is a homopolymer of chlorotrifluoroethylene. It has a chemical structure similar to that of PTFE but with one chlorine atom substituted for a fluorine atom in the repeat group.

Semi finished products are in the form of rod, tube and sheet by extrusion and compression moulding.

### 5.4.2 PROPERTIES

- Unique properties include melt processability excellent chemical resistance.
- Use temperature ranging from  $-240^{\circ}\text{C}$  to  $200^{\circ}\text{C}$
- Low creep and cold flow
- Good ultraviolet stability / High optical transparency
- Low coefficient of thermal expansion
- Excellent electrical insulating properties
- Non-flammability



## 5.5 APPLICATIONS

- PCTFE is an ideal choice for many critical applications in the chemical electrical, electronic, medial and mechanical equipment fields.
- Value seats, seats, gaskets, sight glasses, laboratory equipment, medical equipment, and electronic equipment.
- Mechanical components for example gears, cams bearings and many more....
- The properties of PCTFE moulding materials are specified in ASTM D 1430 and the properties of finished products are specified in SAC AMS 3650

## 5.6 CHEMICAL RESISTANCE

PCTFE is unaffected by most corrosive chemical and most organic solvents. With some halogenated and aromatic compounds slight swelling does occur.

The information listed above is only a small selection of the technical information available about this product for more detailed and extensive information please consults the Fluorocarbon company technical department.

Specific gravity (H-WI-28)	2.08 – 2.18
Tensile strength (H-WI-28)	40 MPa
Elongation (H-WI-28)	90%
Shore D Hardness (ASTM D2240)	75-90
Strength time (ASTM D 1430)	
Compression moulded	200 seconds
Injection moulded	130 seconds
Extruded sections	100 seconds

# Dielectric Properties of Semicrystalline Polychlorotrifluoroethylene (PCTFE) [40]

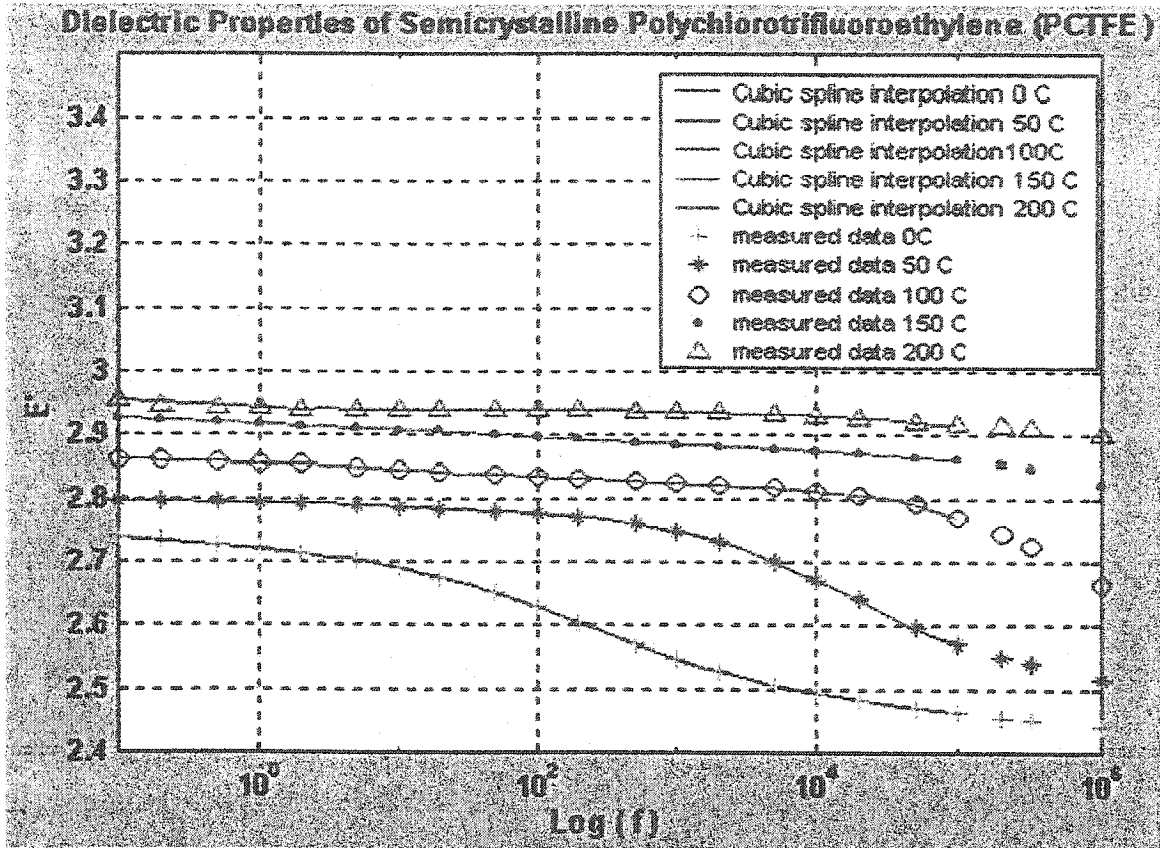


Figure 5.4 Dielectric Properties of PCTFE

## CHAPTER 6

### RESULTS

#### 6.1 COMPARISON WITH THEORITICAL DEBYE CURVES

To test the accuracy of the proposed technique it was applied to theoretical Debye curves where one knows what the resultant Hilbert transform should be.

##### Case 1

$$\varepsilon_s = 80.4$$

$$\varepsilon_\infty = 4.1$$

$$\tau = 1.26 \times 10^{-3} \text{ S}$$

$$f = (0 \text{ to } 10000) \text{ Hz with number of equally spaced samples } N = 8192 (2^{13})$$

It can be clearly seen that  $\hat{\varepsilon}'(\omega)$  is indeed a good approximation to  $\varepsilon''(\omega)$  with some little error existing in the low frequency region of plots. Fig (6.1)

##### Case (11)

Number of sample values increased to 16324 and test the results in this case error were significantly reduced. Fig (6.2)

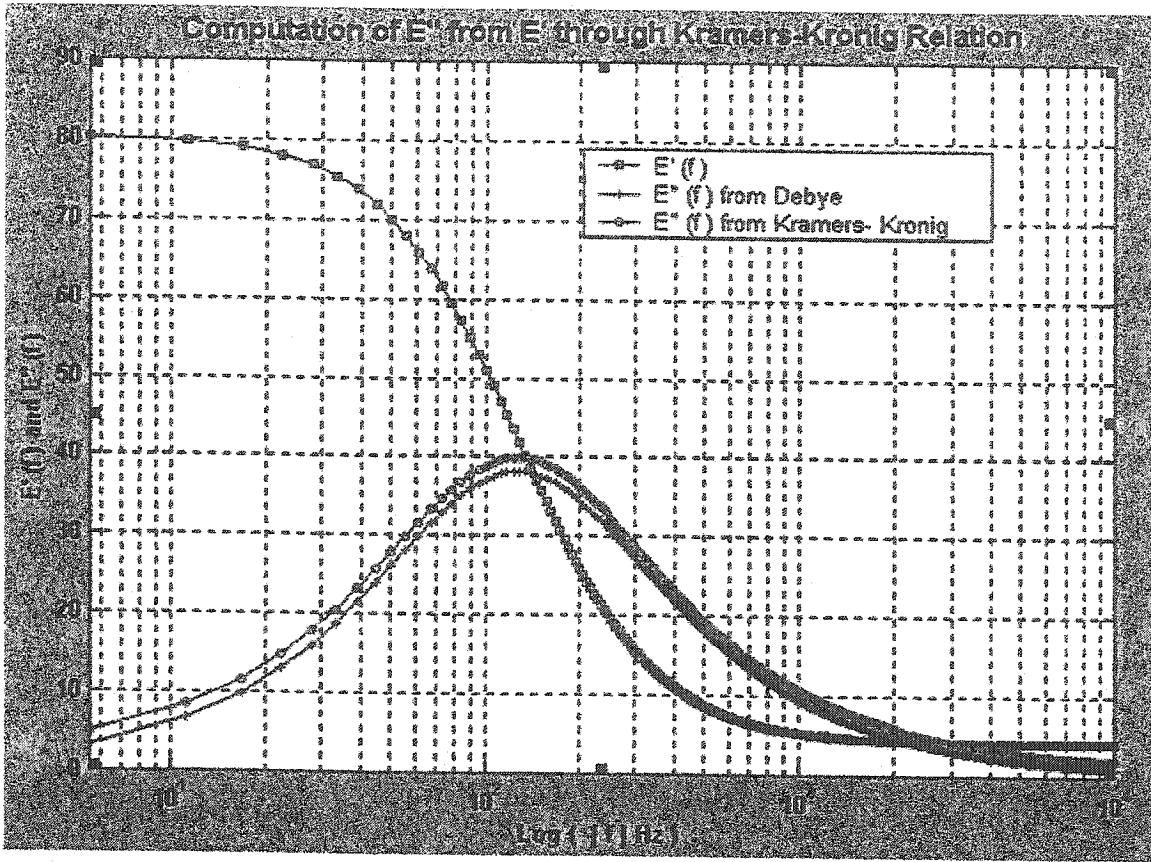


Figure 6.1 Computation of Imaginary part of the Dielectric constant from its Real part (N= 8192 )

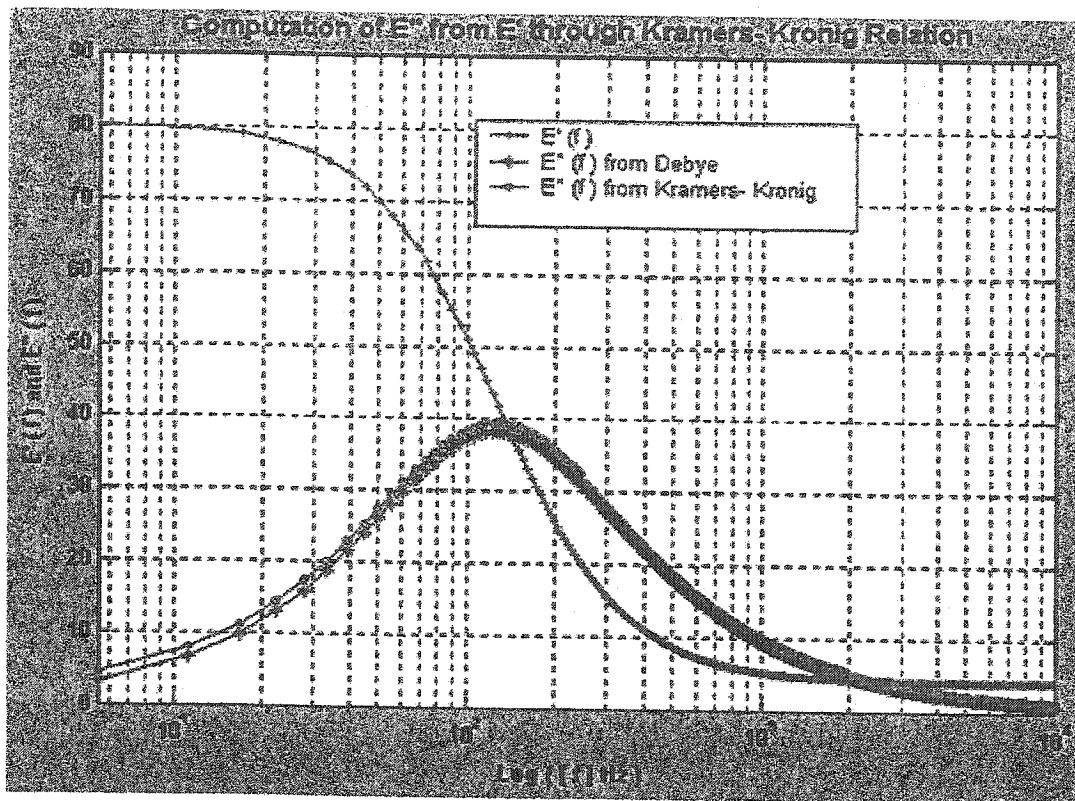


Figure 6.2 Computation of Imaginary Part of the Dielectric constant from its Real part (N=16324)

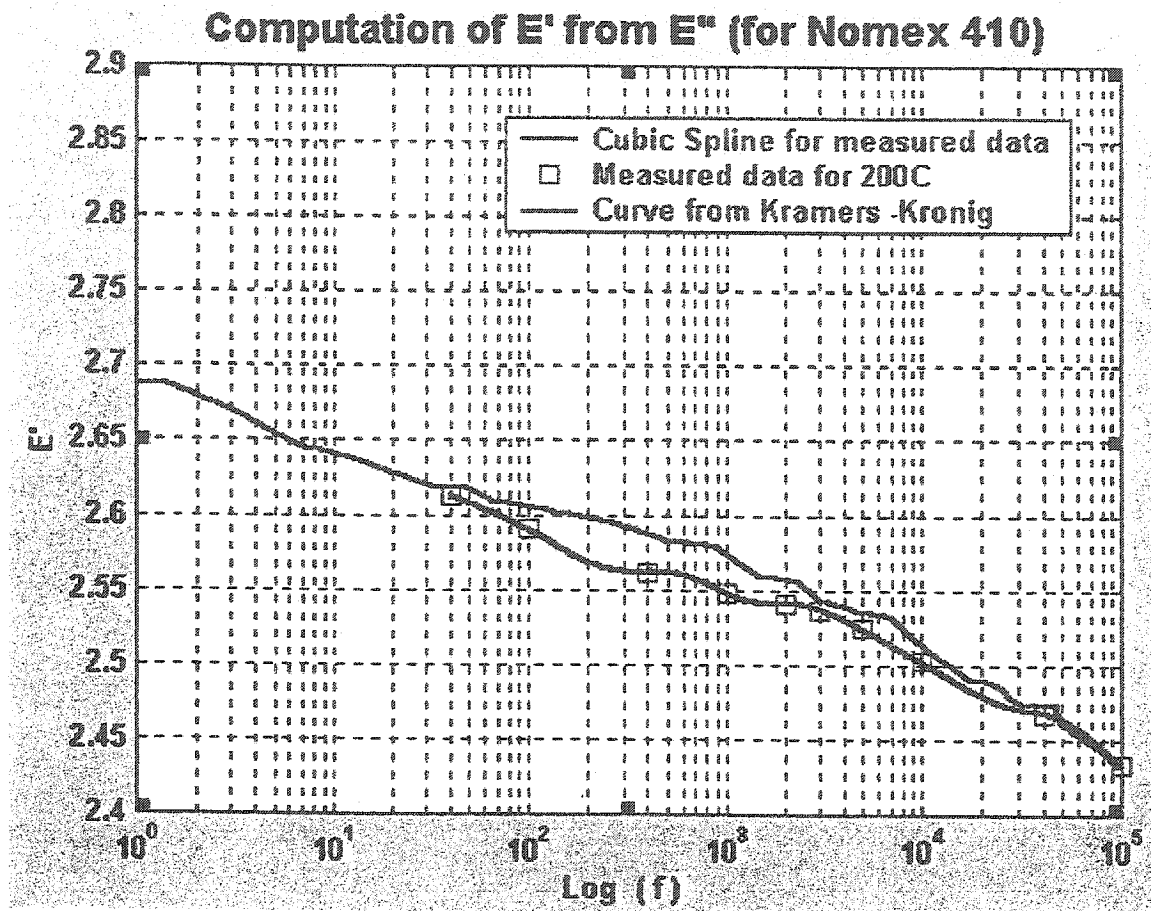


Figure 6.3 Computation of  $E'$  from  $E''$  (NOMEX 410)

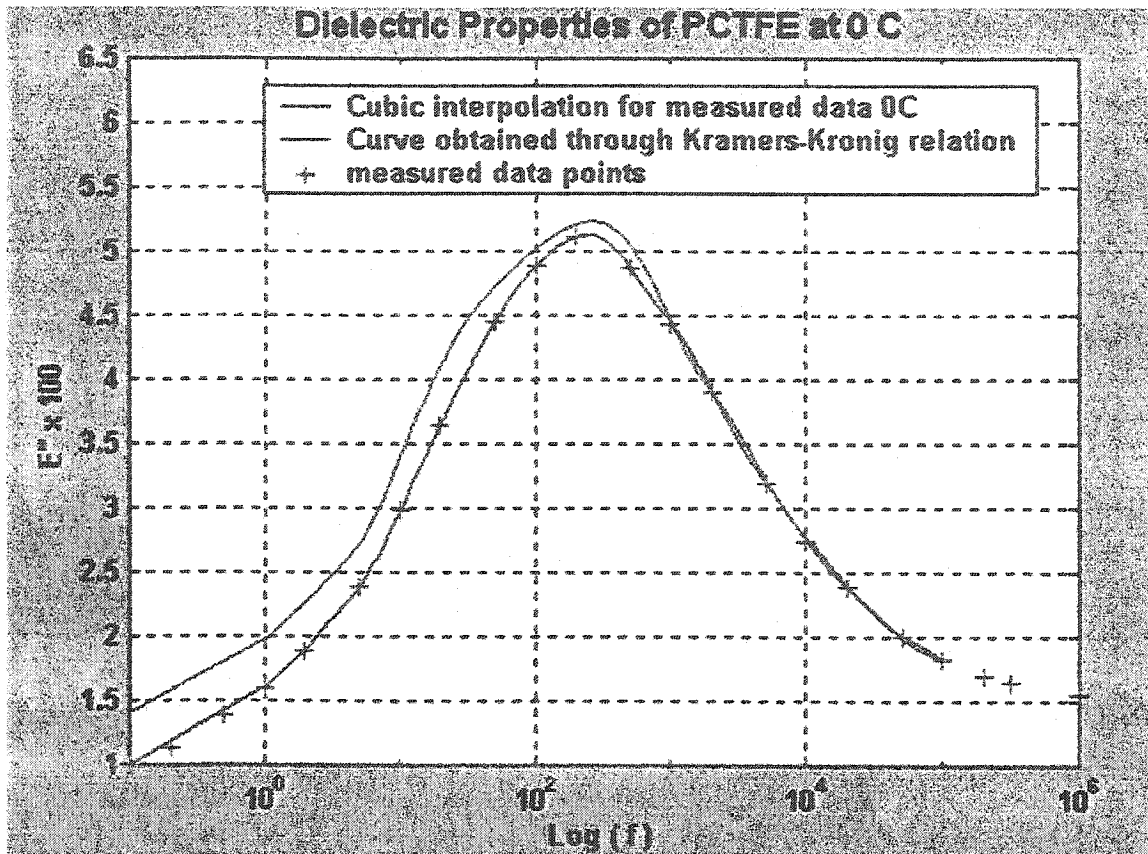


Figure 6.4 Dielectric Properties of PCTFE at 0 C

## CHAPTER 7

### CONCLUSIONS AND RECOMMENDATION FOR FUTURE WORK

The concluding remarks and suggestions for future work are summarized in this chapter. In this thesis it has been shown that the one component of the dielectric constant can be numerically obtained for a large frequency range if its other component is known or measured.

In this thesis an efficient algorithm is developed to obtain one component of the dielectric permittivity of materials over a large frequency range if the other component is known or measured. The algorithm is tested for both theoretically generated data (Debye equation) and measured data for various materials.

The results show that the application of Hilbert transform technique does generate accurate data through this algorithm.

However slight variations arise in low frequency ranges where the experimental values change rapidly. This problem is inherent to the frequency domain based Hilbert transform computation and the complex relaxation behaviour of materials at very low frequencies.

Further, I would like to extend this technique for my research work towards optical properties of semi-conductor materials are not experimentally determined but instead are mathematically computed. This would lead us one step closer to being able to fully model variations in the optical parameters of high-speed photonic devices.



## Appendix

### Preparation of MATLAB Software for Numerical Computations of Dielectric properties

#### Case 1. Theoretical Debye Curves

- a. Introduction of Frequency Range.  
f = [initial value: step :final value ] ;  
f = [0:1.5 :10000]; (say)

- b. Calculation of negative values

F1 = [-10000:1.5:0]; (say)

- c. Introduction of a new array to make periodic signal  
F2 = [F1 f];

- d. Calculation of  $\epsilon'$  using Debye Equation

Relaxation time = Tau =  $1e^{-3}$  (for an example )

$\epsilon_s = 80.4$ ;

$\epsilon_\infty = 4.1$

Num = ( $\epsilon_s - \epsilon_\infty$ ) ;

Cons =  $4 * \pi * \pi * \text{Tau} * \text{Tau}$  ;

Term 1 = cons \* f. ^2 ;

D = 1 + Term 1 ;

C = (d.\*1).^ -1 ;

$\epsilon' = C * \text{Num}$  ;

Sub Plot (311)

Plot (f,  $\epsilon'$ ) ;

- e. Preparation of the  $\epsilon'$  as periodic signal.

E12 = flipir ( $\epsilon'$ ) ;

Sub Plot (312)

Plot ( F1,E12 );

E = [ $\epsilon'$  E12 ] ;

Plot (F2, E ) ; (This gives Full periodic signal )

f. Sampling the signal

```
Del_T = 8 * 2e4 ;  
Tau2 = 2e4;  
M=15;  
N_Tau = 2^M ;  
  
N= N_Tau* ( Del_T/Tau2 );  
Del = Del_T/N_Tau;  
Del_t = Del_T/N  
DEL_F =1/Del_F/N  
N= 0:1:N-1;  
t = n*Del_f;
```

g. Inverse Fourier Transformation.

```
Ein_f = ifft (E );  
Sub Plot (313 )  
Plot (t(1:2000) , abs (Ein_F (f (1 :2000 )) );
```

h. Hilbert Transformation.

```
Eout_1 = Ein_f .* -j  
  
Eout_2 = Ein_f .* j  
  
Eout = [ Eout_1 Eout_2 ] ;
```

i. Fourier Transformation

```
E final = Del_t * fft (Eout );  
  
Sub Plot (314 );  
  
Plot ( F2(1: 13000 ) , abs (E final ( 1 :13000 )) ) – Final Results for Loss factor  
From Dielectric Constant
```

## Case 2. Practical Situations: (Laboratory Measurements)

a. Available Data :

F1 = Frequency = [a1,a2,.....az ]; z- number of data points  
E2 = Loss factor =[ b1,b2,.....bz];

b. Preparation of Spline Curve :

Fx = [0 : Step delta F : Final frequency ] ;  
Ex = Spline [F1,E2,Fx ];

c. Negative Signal Preparation :

F-x = [-Final frequency :Delta F : 0 ];  
E-x = Flipr (Ex ) ;

d. Preparation of Periodic Signal

F= [ F-x Fx ];  
E = [E-x Ex ];

Procedure for f,g,h,and i are as in Debye curves.

## References

- [1] Gorur G. Raju, " Dielectrics in Electric Fields", 2003, Marcel Dekker Inc., New York.
- [2] Harry L. Saums. " Materials for Electrical Insulating and Dielectric Functions", Haden book company, IN, USA, 1973.
- [3] S. Yasufuku, M. Todaki. " Dielectric and thermo analytic Behaviour of moisture and water in Aromatic polamide paper", IEEE Trans. Electrical Insulation, vol 28 No 3, June 1993, pp 228-230.
- [4] G.W. Milton, D.J.Eyre and J.V. Mantese, "Finite Frequency range Kramers-Kronig relations: Bounds on Dispersion" physical Review letters, vol 79, 1997, pp 3062- 3065.
- [5] J.A. Kong, "Electromagnetic wave theory", Wiley & Sons, New York, 1990.
- [6] P.C. Fanning, A. Molina, S.W. Charles, "On the generation of complex susceptibility data through the use of the Hilbert transform", Journal of Physics D, Applied Physics, vol 26,1998, pp 2006-2009.
- [7] J. Bertie, S. Zang, Infrared intensities of liquids IX. The Kramers- Kronig transforms and its approximation by the finite Hilbert transform via fast Fourier transforms. Canadian Journal of Chemistry, vol 70 (2), 1972, pp 520 – 539.
- [8] H. Boche, M. Protzmann, "A new algorithm for the reconstruction of bandlimited functions and their Hilbert transform", IEEE transactions on Instrumentation and measurement, vol 46 (2), 1997, pp 442 – 444.
- [9] J. Vandeschueren and A. Linkens, " Nature of Transient Currents in polymers", J.Appl.phys,vol 49, No7, 1978, pp 4195-4205.
- [10] H.J. Wintle, " Engineering Delectrics", edited by R. Barkitas, Chapter 6, Volume iiA,1983, pp 588-600.
- [11] H. Dishan, " A Wavelet-based algorithm for the Hilbert transform", Mechanical Systems and Signal processing, vol 10 (2), 1996, pp125 –134.

- [12] F.I. Mopsik, "The transformation of Time-domain Relaxation data into the frequency Domain" IEEE transactions on Electrical Insulation vol. EI-20, No 6, Dec 1985, pp 957-964.
- [13] P.J. Hyde, "Wide frequency range Dielectric spectrometer" Proc. IEEE vol. 117, 1970, pp 1891 –1901.
- [14] J.H.Ahlberg, E.H. Nilson and J.L. Walsh, "The theory of Splines and their applications", Academic press NY, 1967.
- [15] K.S.Cole and R.H.Cole "Dispersion and Absorption in Dielectrics (ii) Direct Current characteristics" J. Chem. Phy vol 10, 1942, pp 98 – 105.
- [16] J.V. Cooley and J.W.Turkey, "An algorithm for the Machine Calculation of complex Fourier Series" Math. Com., vol. 19, 1965, pp 297 – 301.
- [18] W.T. Shugg, "Handbook of Electrical and Electronic insulating materials" Wiley Interscience, Second edition, New York, 1995.
- [19] G. R.G .Raju "Conduction and thermally Simulated Discharge Currents in Aramid Paper", IEEE Transactions on Electrical Insulation, vol 27, No 1, Feb 1992, pp 162 – 172 .
- [20] H. J. Wintle "Absorption Currents and Steady Currents in Polymer Dielectrics" J. Non-Crist. Solids, vol 15, 1974, pp 471-486.
- [21] J. Vanderschureren and A. Linkens, "Nature of Transient Currents in Polymers" J. Appl. Phys., vol 49, No 7, 1978, pp 4195 – 4205.
- [22] D.K. Dasgupta, K.Doughty and R.S. Brockley, "Charging and discharging current in polyvinyldine Fluroride". J. Phys., vol 113, 1980, pp 2101 – 2114.
- [23] B.V. Hamon. "An approximate Method to deducing dielectric loss factor from direct current measurement" Proc. IEE (London), vol 99, 1952, pp 151 – 155.
- [24] Baird M.E., "Derermination of Dielectric behavior at low frequencies form measurement of anomalous charging and discharging current" Review of Modern Physics, vol 140, 1968, pp 219 – 227.

- [25] Technical Specification Guide Keithley 617C VRL:  
<http://www.keithley.com>
- [26] M.A. Sussi and G.R.Govinda Raju “Absorption and Thermally Stimulated Polarization Current in Aramid Paper” SAMPE Journal, vol 28, No 4, 1992
- [27] M.A.Sussi, “Charge Storage and Decay in High temperature Insulating Materials”, PhD Thesis, University of Windsor, ON, Canada, 1992.
- [28] A.K. Jonscher “ The Universal Dielectric response Conference on Electrical Insulation and Dielectric Phenomena Pocono Manor P A, Oct 28 1990, pp 23-40.
- [29] Saeed-Ul-haq “Relaxation and Brakedow Studies in High Temperature Dielectrics” M.A.Sc. Thesis, University of Windsor, ON, Canada, 2001.
- [30] Daniel V.V. “Dielectric Relaxation” (London Academic ), 1967.
- [31] Debye P. “Polar Molecules (Newyork, Chemical Catalogue Company), 1929.
- [32] Paul B. Crilly “An Introduction to Signels and Noise in Electrical Communication”, 4<sup>th</sup> edition, C.Britton Rorabaugh, McGraw-Hill, USA, 2000.
- [33] Leon W. E. “Digital and Analog Communicaiton Systems”, 6<sup>th</sup> Edition, Thompson Asia Ltd., Singapore, 2000
- [34] Riaz R. Shaikh “Electrical Conduction in Dielectric Films” M.A.Sc. Thesis, University of Windsor, ON, Canada, 2002.
- [35] Roden M.S. “Analog and Digital Communication Systems (London, Prentice – Hall), 1991.
- [36] Z. Leo Wu, G.R.G. Raju Electrical Conduction in Fluropolymer Films IEEE trans Electrical Insulation, vol 2 , June 1995, pp 475 – 482.
- [40] Arnold H. Scott “ Dielectric Proerties of SemiCrystalline Polychlorotrifroethylene” Journal of Research National B. S. Phy & Che, vol 66A, No (4), Aug 1962.
- [41] H.R. Phillipp and H. Ehreneich “ Optical properties of Semi Conductors “ Physical Review, vol 129, No 4, 1963 , pp 1550 – 1560.

- [42] H. Frohlich "Theory of Dielectrics", Oxford University Press, London, 1958.
- [43] B. Gross " On the theory of Dielectric Loss" Physical Review, vol 59, 1941, pp 748.
- [44] F.M.Clark "Insulating Materials for Design and Engineering Practice" John Wiley and Sons., London,1962, pp 466 – 505.
- [45] H.J.Wintle, IEEE trans Elect. Insulation EI-120, 1977, pp 424.
- [46] S. Havriliak and D.G.Watts, Polymer, vol 27, 1986, pp 1509 – 1512.
- [47] R- Nozaki, J. Chem physics, vol 87, 1987, pp 2271
- [48] D.W.Davidson and R.H.Cole, J. Che physics, vol 19, 1951, pp1484 – 1490.

## VITA AUCTORIS

**NAME:** Ruwan D. Weerasundara

**DATE OF BIRTH:** 14<sup>TH</sup> January 1962

**PLACE OF BIRTH:** Kandy, Central Province, Sri- Lanka

**EDUCATION:**

- 1981 – 1987 University of Peradeniya  
Sri Lanka (B.Sc. Electrical Engineering)
- 1990 – 1991 University of Twente, The Netherlands  
(Diploma in Energy Management )
- 2002 – 2003 University of Windsor, Ontario, Canada  
(Master of Applied Science – Electrical  
Engineering)

**WORK HISTORY:**

- 1987 – 1989: Trainee Engineer  
Lanka Electricity Company (Pvt) Ltd.  
Colombo, Sri Lanka.
- 1989 – 1992: Operations Engineer  
Canyon Hydro Power Station  
Ceylon Electricity Board,  
Maskelliya, Sri Lanka.
- 1992 – 1996: Distribution Design Engineer  
Ceylon Electricity Board,  
Colombo, Sri Lanka.
- 1996 – 2000 Chief Engineer (Distribution Design)  
Ceylon Electricity Board,  
Colombo, Sri Lanka.
- 2001 – 2002 Power Distribution Design Engineer  
Professional Engineering Services,  
Detroit, USA.